EXPLORING THE RELATIONSHIP BETWEEN TOXIN AND SPORE PRODUCTION IN THE HUMAN ENTERIC PATHOGEN *CLOSTRIDIUM DIFFICILE*

SARA DE CASTRO GONÇALVES RAMALHETE

A THESIS SUBMITTED FOR THE DEGREE OF MASTER IN MEDICAL MICROBIOLOGY

OCTOBER, 2015

EXPLORING THE RELATIONSHIP BETWEEN TOXIN AND SPORE PRODUCTION IN THE HUMAN ENTERIC PATHOGEN *CLOSTRIDIUM DIFFICILE*

SARA DE CASTRO GONÇALVES RAMALHETE

A THESIS SUBMITTED FOR THE DEGREE OF MASTER IN MEDICAL MICROBIOLOGY

Supervisor: Prof. Dr. Adriano O. Henriques

Co-supervisor: Dr. Mónica Serrano

Experimental work performed at the *Instituto de Tecnologia Química e Biológica António Xavier/ UNL*, Av. da República, Estação Agronómica Nacional 2780-157 Oeiras, Portugal.

OCTOBER, 2015

Bibliographic elements resulting from this dissertation

Oral papers:

Carolina P. Cassona, Sara Ramalhete, Wilson Antunes, Bruno Dupuy, Mónica Serrano and Adriano O. Henriques. June 2015. The link between toxinogenesis and sporulation during infection by the human intestinal pathogen *Clostridium difficile.* 17TH European workshop on bacterial protein toxins. Braga, Portugal.

Carolina P. Cassona, Sara Ramalhete, Wilson Antunes, Bruno Dupuy, Mónica Serrano and Adriano O. Henriques. September 2015. The link between toxin production and spore formation in the intestinal pathogen *Clostridium difficile*. Clostpath 2015 – 9TH International conference on the Molecular Biology and Pathogenesis of the Clostridia. Freiburg, Germany.

Posters:

Carolina P. Cassona, Sara Ramalhete, Wilson Antunes, Bruno Dupuy, Mónica Serrano and Adriano O. Henriques. October 2015. The link between toxinogenesis and sporulation during infection by the human intestinal pathogen *Clostridium difficile.* 1º Workshop of Genetics. Lisbon, Portugal.

Acknowledgements

First, I would like to thank Prof. Dr. Adriano O. Henriques and Dr. Mónica Serrano for the opportunity to work in the laboratory and for the guidance they provided me every time that I needed. They were always available to discuss ideas and to give me constructive criticisms, which were crucial for me to learn and think outside the box.

I also would like to thank Carolina Cassona, a very hard worker PhD student that was always ready to help and to dispense some of her time to teach me new techniques, and to all of the MDL colleagues, Aristides Mendes, Carolina Feliciano, Hugo Barreto, Inês Portinha, João Bota, Patrícia Amaral and Wilson Antunes, which were very important to turn the team work into funny and pleasant moments. Also, to Teresa Silva for all the help in routinary tasks which were crucial for me to save some time.

I would like to thank the Scientific Committee of the MSc in Medical Microbiology of UNL for the organization of this master's course and to *Instituto de Tecnologia Química e Biológica António Xavier* of *Universidade Nova de Lisboa* for receiving me as a master student during this year.

Moreover, I would like to thank my family, Rui Ramalhete, Manuela Ramalhete and Rui Miguel Ramalhete, for the constant support they gave me to proceed my dreams and reach success. To David Braz, which was always ready to give me comfort words that were pivotal for me to be the best that I could and for all the good moments that turned this journey even happier.

Finally, to all of my friends which are also family and helped me to relax and create great memories during the last year.

Abstract

Clostridium difficile is currently the major cause of antibiotic-associated gastrointestinal diseases in adults. This is a Gram-positive bacterium, endospore-forming and an obligate anaerobe that colonizes the gastrointestinal tract.

Recent years have seen a rise in *C. difficile* associated disease (CDAD) cases, associated with more severe disease symptoms, higher rates of morbidity, mortality and recurrence, which were mostly caused due to the emergence of "hypervirulent" strains but also due to changing patterns of antibiotics use. *C. difficile* produces two potent toxins, TcdA and TcdB, which are the main virulence factors and the responsible for the disease symptoms. These are codified from a Pathogenicity Locus (PaLoc), composed also by the positive regulator, TcdR, the holin-like protein, TcdE, and a negative regulator, TcdC. Besides the toxins, the oxygen-resistant spores are also essential for transmission of the organism through diarrhea; moreover, spores can accumulate in the environment or in the host, which will cause disease recurrence.

The expression of the PaLoc genes occurs in vegetative cells, at the end of the exponential growth phase, and in sporulating cells. In this work, we constructed two in-frame deletion mutants of *tcdR* and *tcdE*. We showed that the positive auto regulation of *tcdR* is not significant. However, *tcdR* is always necessary for the expression of the PaLoc genes.

A previous work showed that, except *tcdC*, all the PaLoc genes are expressed in the forespore. Here, we detected TcdA at the spore surface. Furthermore, we showed that the in-frame deletion of *tcdE* does not affect the accumulation of TcdA in the culture medium or in association with cells or spores. This data was important for us to conclude about the infeccious process: it suggests that the spore may be the vehicle for the delivery of TcdA in early stages of infection, that TcdA may be released during spores germination and that this spore may use the same receptor recognized by TcdA to bind to the colonic mucosa.

Resumo

Clostridium difficile é presentemente a principal causa de doença gastrointestinal associada à utilização de antibióticos em adultos. *C. difficile* é uma bactéria Gram-positiva, obrigatoriamente anaeróbica, capaz de formar endósporos. Tem-se verificado um aumento dos casos de doença associada a *C. difficile* com sintomas mais severos, elevadas taxas de morbilidade, mortalidade e recorrência, em parte, devido à emergência de estirpes mais virulentas, mas também devido à má gestão do uso de antibióticos. *C. difficile* produz duas toxinas, TcdA e TcdB, que são os principais fatores de virulência e responsáveis pelos sintomas da doença. Estas são codificadas a partir do Locus de Patogenicidade (PaLoc) que codifica ainda para um regulador positivo, TcdR, uma holina, TcdE, e um regulador negativo, TcdC. Os esporos resistentes ao oxigénio são essenciais para a transmissão do organismo e recorrência da doença.

A expressão dos genes do PaLoc ocorre em células vegetativas, no final da fase de crescimento exponencial, e em células em esporulação. Neste trabalho construímos dois mutantes de eliminação em fase dos genes *tcdR* e *tcdE*. Mostrámos que a auto-regulação do gene *tcdR* não é significativa. No entanto, *tcdR* é sempre necessário para a expressão dos genes presentes no PaLoc.

Trabalho anterior mostrou que, com a exceção de *tcdC*, os demais genes do PaLoc são expressos no pré-esporo. Mostrámos aqui que TcdA é detectada à superfície do esporo maduro e que a eliminação do *tcdE* não influencia a acumulação de TcdA no meio de cultura ou em associação às células ou ao esporo. Estas observações têm consequências para o nosso entendimento do processo infecioso: sugerem que o esporo possa ser também um veículo para a entrega da toxina nos estágios iniciais da infecção, que TcdA possa ser libertada durante a germinação do esporo, e que o esporo possa utilizar o mesmo receptor reconhecido por TcdA para a ligação à mucosa do cólon.

Table of contents:

List of Figures

List of Tables

Page

Symbols and Abbreviations

: :	Interruption/junction
°C	Degree centigrade
A	Ampere
A	Absorbance
bp	Base pair
cfu	Colony-forming unit(s)
DNA	Deoxyribonucleic acid
DNase	Deoxyribonuclease
DTT	Dithiothreitol
EDTA	Ethylenediaminetetraacetic acid
g	Acceleration of gravity
g	Gram
GTP	Guanosine triphosphate
h	Hour
kDa	Kilodalton
L	Liter
M	Molar
mg	Milligram
min	Minutes
ml	Mililiter
mM	Millimolar
ms	Millisecond
PBS	Phosphate-buffered saline
PCR	Polymerase chain reaction
RNA	Ribonucleic acid
RNAse	Ribonuclease
SDS	Sodium dodecyl sulfate

PAGE	Polyacrylamide gel electrophoresis
PMSF	Phenylmethylsulfonyl fluoride
Tris	Tris(hydroxymethyl)aminomethane
UV	Ultraviolet
v	Volume
V	Volt
WT	Wild type
Δ	Deletion
nM	Nanomolar
μg	Microgram
μl	Microliter
μm	Micrometer
μM	Micromolar
σ	Sigma

The abbreviations listed are according to the recommendations published by the Journal of Biological Chemistry (JBC). All the other abbreviations are defined in the text.

1. Introduction

1.1. *Clostridium difficile*

Clostridium difficile is currently the major cause of antibiotic-associated gastrointestinal diseases in adults (Rupnik *et al.*, 2009). *C. difficile* is a Gram-positive bacterium, endospore-forming (hereinafter named spore for simplicity) and an obligate anaerobe that colonizes the gastrointestinal tract. *C. difficile* infection (CDI) occurs when the gut microbiota is disrupted (Jernberg *et al.*, 2010; Willing *et al.*, 2011; Pérez-Cobas *et al.*, 2013a; Figure 1) and has a range of consequences from asymptomatic carriage to toxic megacolon, bowel perforation, sepsis, septic shock and death (Rupnik *et al.*, 2009).

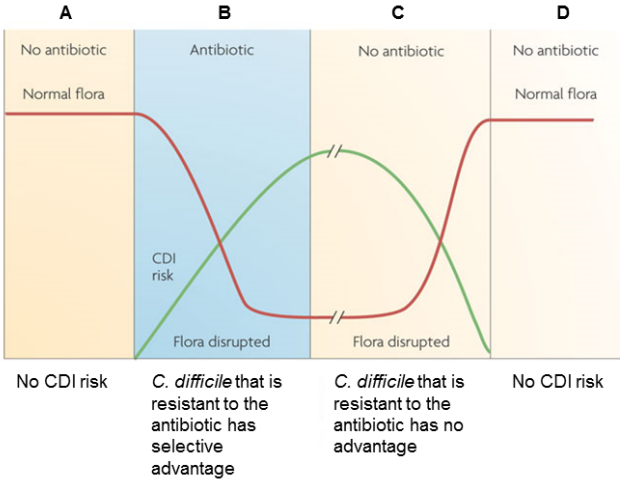

Figure 1- Development of *C. difficile* disease. A: Patients are resistant to CDI if their normal microbiota is not disrupted by antibiotics; B: Once antibiotic treatment starts, infection with a *C. difficile* strain that is resistant to the antibiotic is more likely; C: When the antibiotic treatment stops, the levels of the antibiotic in the gut diminish rapidly, but the microbiota remains disturbed for a variable period of time (indicated by the break in the graph), depending on the antibiotic given; D: During this time, patients can be infected with either resistant or susceptible *C. difficile*. Finally, after the microbiota recovers, the resistance to *C. difficile* is restored (Adapted from Rupnik *et al.*, 2009).

Recent years have seen a rise in C. *difficile* associated disease (CDAD) cases, associated with more severe disease symptoms, higher rates of morbidity, mortality and recurrence, in part because of the emergence of so called hypervirulent strains, mainly, but not exclusively of a specific ribotype, termed 027 (McDonald *et al.*, 2005). Changing patterns of antibiotic use have contributed to the problem (McFarland *et al.*, 2007). While most CDAD cases affect hospitalized patients under antibiotic treatment, in particular clindamycin, aminopenicillins, cephalosporins and fluoroquinolones (Johnson *et al.*, 1999; Gaynes *et al.*, 2004; Loo *et al.*, 2005; Muto *et al.*, 2005; Pépin *et al.*, 2005), cases

have also been reported without any relation to health care facilities or administration of antibiotics prior to the diagnosis (Rupnik *et al.*, 2009). Therefore, CDI is a growing concern at the community level, as well as in animal husbandry (Rodriguez-Palacios *et al.*, 2006; Songer and Anderson, 2006; Rupnik, 2007).

C. difficile produces two potent toxins, TcdA and TcdB, which are the main virulence factors and the main causes of the disease symptoms (Rupnik *et al.*, 2009; Burns *et al.*, 2010; Carter *et al.*, 2012; Deakin *et al.*, 2012; Sarker and Paredes-Sabja, 2012). However, the oxygen-resistant spores are essential for transmission of the organism; moreover, spores can accumulate in the environment, and in the host, and are responsible for disease recurrence (Rupnik *et al.*, 2009; Burns *et al.*, 2010; Carter *et al.*, 2012; Deakin *et al.*, 2012; Sarker and Paredes-Sabja, 2012). Infection generally begins with the ingestion of spores; ingested spores will reach the anaerobic colon and germinate. *C. difficile* responds to unique germinants, such as bile salts (Wilson, 1983). While the bile salt cholate (CA) induces spore germination, another primary bile salt, chenodeoxycholate (CDCA) has been identified as a potent inhibitor of the process (Sorg and Sonenshein, 2008a and b). Upon antibiotic administration, the metabolism of these two compounds is altered and the CA concentration in the gut becomes higher than CDCA, triggering spore germination (Giel *et al*., 2010). As the organism propagates, it can produce the TcdA and TcdB cytotoxins and more spores (Deneve *et al.*, 2009; Carter *et al.*, 2012). TcdA and TcdB are Rho-glucosylating toxins that cause very typical inflammatory lesions in the colon epithelium, called pseudomembranes (Just *et al.*, 1995; Thelestam and Chaves-Olarte, 2000; Jank *et al.*, 2007; Rupnik *et al.*, 2009). Damage of the colonic mucosa eventually leads to severe diarrhea, which allows shedding of the spores and transmission to new hosts. The treatment recommended by the European Society of Clinical Microbiology and Infectious Diseases (ESCMID) is based on the administration of vancomycin, metronidazole and the recently introduced fidaxomicin; however, these antibiotics may lead to dysbiosis (Debast *et al.*, 2014). Moreover, strains resistant to vancomycin and metronidazole have been isolated (Dworczyński *et al.*, 1991; Pelaez *et al.*, 1994).

The severity of the disease seems linked to the level of dysbiosis (Jernberg *et al.*, 2010; Willing *et al.*, 2011; Pérez-Cobas *et al.*, 2013a). While the microbiota may have an overall protective role, some species-specific interactions may be important to maintain *C. difficile* in check. A recent study shows that the germination of *C. difficile* spores is

inhibited by *C. scindens*; this occurs because *C. scindens* is capable of modifying endogenous bile salts which are potent triggers of *C. difficile* spore germination (Buffie *et al.*, 2015). Therefore, and due to the emerging resistant strains, alternative therapies, as the faecal microbiota transplantation, are being consider (Matsuoka *et al.*, 2014).

1.2. Sporulation

Spores are central for the pathogenesis of *C. difficile*. Spores are highly resistant dormant cell types and this resistance is related to their functional architecture. The genome is contained within a central compartment delimited by a lipid bilayer with a layer of peptidoglycan (PG) (germ cell wall) apposed to its external leaflet; this PG layer will serve as the wall of the outgrowing cell that forms when the spore completes germination (Henriques and Moran, 2007; de Hoon *et al.*, 2010; McKenney *et al.*, 2012). The germ cell wall is surrounded by a modified form of PG, called cortex that is essential for the acquisition and maintenance of spore heat resistance (Henriques and Moran, 2007; McKenney *et al*, 2012). In turn, the cortex is enveloped in a multiprotein coat normally differentiated into two main layers, an inner and an outer coat. In some organisms, including the pathogens *B. anthracis*, *B. cereus* and most likely *C. difficile*, the coat is further enclosed within a structure known as the exosporium. The exosporium is formed by a basal layer from where projections of glycosylated collagen-like proteins emanate (Sylvestre *et al.*, 2002; 2003; Steichen *et al.*, 2003). The coat and exosporium protect the spore cortex from the action of PG-breaking enzymes produced by host organisms or predators, and confer protection to radiation, UV light and small toxic molecules. In addition, the spore surface layers, are required for normal recognition of the molecules that signal spore germination and also mediate spore adhesion to cells and abiotic surfaces (Henriques and Moran, 2007; Panessa-Warren *et al.*, 2007; Oliva *et al.*, 2009; Paredes-Sabja *et al.*, 2012; Paredes-Sabja and Sarker, 2012).

The process of spore differentiation has been extensively studied in the model organism *B. subtilis* but the main morphological stages of sporulation are common to other endospore formers that have been studied in some detail (Henriques and Moran, 2007; de Hoon *et al.*, 2010; McKenney *et al.*, 2012). A hallmark of sporulation is an asymmetric (polar) division that divide the rod-shaped cell into a larger mother cell and a smaller forespore, the future spore. The mother cell then engulfs the forespore and this

process isolates the forespore from the surrounding medium, releasing it as a cell, surrounded by a double membrane, within the mother cell cytoplasm (Hilbert and Piggot, 2004; Higgins and Dworkin, 2012). With the exception of the germ cell wall, which is formed from the forespore, the assembly of the main spore protective structures is mostly a function of the mother cell (Henriques and Moran, 2007; McKenney *et al.*, 2012). At the end of the process, and following a period of spore maturation, the mother cell undergoes autolysis, to release the mature spore (Figure 2).

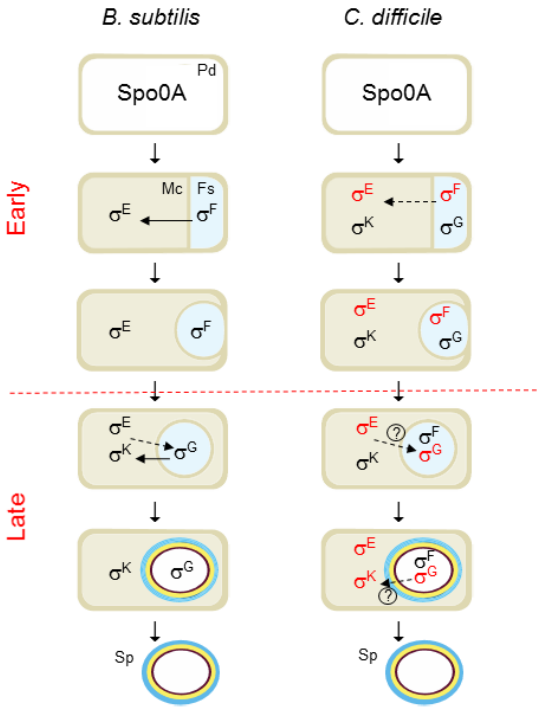

Figure 2 - Morphological stages and compartmentalized gene expression of *B. subtilis* and *C. difficile* sporulation. In a nutrient rich medium, the cell grows and divides by symmetric division (Predivisional cell, Pd). However, upon starvation, the cell enters in sporulation. The process begins with an asymmetric cell division, then, the mother cell (Mc) membrane migrates around the forespore (Fs), engulfing it. At the end of this process, the forespore becomes a free protoplast in the mother cell cytoplasm. Finally, the cortex (brown) and coat (yellow and blue) layers are synthesized and deposited around the developing spore (Sp) and, upon mother cell lysis, a mature spore is released to the surrounding environment, where it remains in a dormant state until good germination conditions. The compartment of activity of the sporulation σ^F, σ^E, σ^G and σ^K sigma factors is indicated; their main period of activity in *C. difficile* cells is indicated in red (Pereira *et al.*, 2013).

The developmental regulatory network of sporulation shows a hierarchical organization and functional logic (de Hoon *et al.*, 2010). A master regulatory protein, Spo0A, activated by phosphorylation, governs entry into sporulation, including the switch to asymmetric division (Hilbert and Piggot, 2004; Piggot and Hilbert, 2004). Gene expression in the forespore and mother cell is controlled by 4 cell type-specific sigma factors, which are sequentially activated, alternating between the mother cell and the forespore (Figure 2). When Spo0A-P level reaches a critical threshold in *B. subtilis*, it

activates sporulation genes including *spoIIE* as well as both the *spoIIAA-spoIIAB-sigF* and the *spoIIGA-sigE* operons encoding σ^F and σ^E, respectively (Molle *et al.*, 2003). Regarding the *B. subtilis* model, σ^F and σ^E control the early stages of development in the forespore and the mother cell, respectively, and are replaced by σ^G and σ^K when engulfment of the forespore is completed (Hilbert and Piggot, 2004; Piggot and Hilbert, 2004; Figure 2). The result is the coordinated deployment of the forespore and mother cell lines of gene expression (Hilbert and Piggot, 2004; Piggot and Hilbert, 2004).

The sporulation pathway of *C. difficile* and the underlying genetic regulatory network have been recently characterized (Fimlaid *et at*, 2013; Pereira *et al.*, 2013; Saujet *et al.*, 2013). The main periods of activity of the four cell type-specific sigma factors of *C. difficile* are conserved in comparison with the *B. subtilis* model (Pereira *et al.*, 2013). However, in *C. difficile* the fact that the activity of σ^E was partially independent of σ^F, and that σ^G or σ^K did not require σ^E or σ^G, respectively, seems to imply a weaker connection between the forespore and mother cell lines of gene expression (Pereira *et al.*, 2013). Relatively to the aerobic Bacilli, the Clostridia represent an older group within the Firmicutes phylum, at the base of which endosporulation has emerged some 2.5 billion years ago, before the initial rise in oxygen level in the earth atmosphere (Stragier, 2002; Paredes *et al.*, 2005; Galperin *et al.*, 2012; Miller *et al.*, 2012; Traag *et al.*, 2012; Abecasis *et al.*, 2013).

1.3. Pathogenicity Locus (PaLoc)

The TcdA and TcdB toxins are encoded by genes located in a Pathogenicity Locus, or PaLoc, which carries the genes for three other proteins, TcdR, TcdE and TcdC (Hammond and Johnson, 1995, Figure 3). TcdR is an RNA polymerase sigma factor that serves as the main positive regulator of expression of the PaLoc (Mani and Dupuy, 2001). TcdE is a holin-like protein thought to be involved in toxin secretion (Govind and Dupuy, 2012). TcdC is a putative TcdR-specific anti-sigma factor that negatively regulates *tcdR*-dependent transcription, at least *in vitro* (Matamouros *et al.*, 2007; but see below).

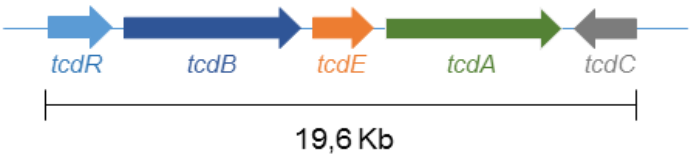

Figure 3 - Schematic image of the Pathogenecity Locus (PaLoc). TcdR is a RNA polymerase sigma factor that acts as the positive regulator for PaLoc expression; TcdA and TcdB are the cytotoxins, TcdE is a holin-like protein and TcdC, a possible anti-TcdR factor (Hammond and Johnson, 1995; Mani and Dupuy, 2001; Matamouros *et al*., 2007; Govind and Dupuy, 2012).

1.3.1. The positive regulator (TcdR) and the "negative" regulator (TcdC)

TcdR is an alternative sigma factor with 22 kDa (Moncrief *et al.*, 1997) that positively regulates toxin production and also activates its own expression (Mani and Dupuy, 2001). This is consistent with the presence of two potential promoters for TcdR-dependent transcription in the region upstream of the *tcdR* gene (Mani *et al.*, 2002). Recently, El Meouche and co-workers identified a third potential promoter upstream of *tcdR* and showed that SigD, the main regulatory protein for flagellar biogenesis and motility, positively controls toxin gene expression (El Meouche *et al.*, 2013). Under what conditions are the *tcdR* promoters utilized is still unclear.

Regarding TcdC, this is an acidic, membrane-associated protein with a predicted molecular weight of 26 kDa (Braun *et al.*, 1996; Govind *et al.*, 2006), which can form dimers (Matamouros *et al.*, 2007). High levels of *tcdC* transcription may occur during the exponential growth phase of *C. difficile* , concomitant with low transcription of *tcdR* and of the *tcdA* and *tcdB* genes, whereas during entry into stationary phase transcription of *tcdC* is low, and transcription of *tcdR* and the toxin genes is high (Hundsberger *et al.*, 1997). The reported inverse correlation between the transcription of *tcdC* and the toxin genes and the expression patterns of the corresponding proteins has led to the prevailing model that TcdC is an important repressor of toxin expression (Hundsberger *et al.*, 1997). This model seems to be supported by the latter finding that the absence of a functional TcdC caused by a frame shift mutation (D117 bp) in the *tcdC* gene is linked to increased toxin production in certain "hypervirulent" strains (Warny *et al.*, 2005; Curry *et al.*, 2007). Importantly, TcdC can bind to TcdR and inhibit TcdR-directed transcription *in vitro*, serving as an anti-sigma factor by destabilizing the TcdR-RNA polymerase core enzyme complex (Matamouros *et al.*, 2007).

However, recently, some doubts were raised about the importance of TcdC for regulation of toxin expression on the basis of several lines of evidence. First, two studies have found increasing levels of *tcdC* transcription in time that coincide with increasing transcription of the toxin genes and increasing amounts of toxin production (Merrigan *et al.*, 2010; Vohra and Poxton, 2011). Second, there is a great variability in toxin expression levels among "hyperirulent" strains, even though these generally carry mutations in *tcdC* (Curry *et al.*, 2007; Merrigan *et al.*, 2010; Vohra and Poxton, 2011). Third, the prevailing model that TcdC is a negative regulator of toxin expression was supported by the finding that introduction of a functional *tcdC* gene into an epidemic strain that carries a non-functional *tcdC* gene (M7404, a PCR ribotype NAP1/027 strain) resulted in decreased toxin production and attenuated virulence in a hamster model (Carter *et al.*, 2011). However, chromosomal complementation in strain R20291, another PCR ribotype NAP1/027 strain with an inactive *tcdC* gene, resulted in no discernible effect on toxin expression (Cartman *et al.*, 2012). Moreover, other studies showed that disruption of the *tcdC* gene in the widely used laboratory strain 630Δ*erm* had little if any effect on toxin expression under the conditions tested (Bakker *et al.*, 2012; Cartman *et al.*, 2012). Fourth, recently, van Leeuwen and co-authors showed that TcdC could bind to DNA folded into G-quadruplex structures containing repetitive guanine nucleotides, suggesting that TcdC might also act by destabilizing the open complex formation before transcription initiation; however, no quadruplex-forming motif with multiple G-stretches was found in the PaLoc (van Leeuwen *et al.*, 2013).

The reasons for the conflicting data may relate to experimental variations, including the strain used or the specific growth conditions, either of which might affect the level of TcdC expression or activity (Bouillaut *et al.*, 2015). In conclusion, TcdC might have a modulatory role in regulating toxin expression, but it is probably not a major determinant of the "hypervirulence" of *C. difficile* (Bakker *et al.*, 2012).

1.3.2. *Clostridium difficile* cytotoxins

TcdA and TcdB are single-chain proteins with molecular masses of 308 and 270 kDa, respectively, that belong to the group of "Large Clostridial Cytotoxins" (Genth *et al.*, 2008).

Two infection studies in hamsters attempted to clarify the roles of TcdA and TcdB in gastrointestinal disease by using isogenic toxin mutants constructed in the low-virulence clinical isolate 630 (Lyras *et al.*, 2009; Kuehne *et al.*, 2010). The first study found that TcdB alone resulted in disease (Lyras *et al.*, 2009), while the second concluded that both TcdB and TcdA could individually cause severe disease (Kuehne *et al.*, 2010). It is interesting to note that a number of clinical cases of *C. difficile* infection have been attributed to naturally occurring $A^{-}B^{+}$ strains (Drudy *et al.*, 2007; 2007), but that there have been no reports of naturally occurring $A^{+}B^{-}$ isolates until now. This would suggest that $A^{+}B^{-}$ strains do not exist, but it may also be an artefact of routine diagnostic testing practices. Either way, if they do not exist in nature already, they may yet evolve.

Thus, both TcdA and TcdB seem to have an enterotoxin activity, however, since TcdB causes several other symptoms outside the gastrointestinal region (Lanis *et al.*, 2013) and has a higher cytopathic potency toward cultured cells (Donta *et al*., 1982), it is more correct to refer this toxin as cytotoxin.

Both toxins are composed by an N-terminally glucosyltransferase domain followed by a cysteine protease domain, a transmembrane domain and a C-terminally receptor binding domain which harbours repetitive peptide elements called "combined repetitive oligopetides" (CROPs) (Genth *et al.*, 2008). These CROPs exhibit homology to either the carbohydrate-binding regions of glycosyltransferases or to domains for the specific recognition of choline-containing cell-wall components (Just and Gerhard, 2004). In fact, it was shown that TcdA binds to the glycoprotein gp96, a member of the heat shock protein family, and that this binding enhances cellular entry of the toxin (Na *et al.*, 2008). Regarding TcdB, Michelle E. LaFrance *et al.* (2015) claim that PVRL3 is one of the receptors since they observed a direct binding interaction between PVRL3 and TcdB using purified proteins (LaFrancea *et al.*, 2015). Furthermore, they showed that PVRL3 is independent of the CROPs. This model is compatible with the dual-receptor mechanism, proposed by Schorch *et al*. (2014) where the CROPs domain allows the toxin to dock onto the cell surface by interacting with oligosaccharides, followed by toxin binding to a high-affinity receptor (Schorch *et al.*, 2014).

Although there are some potential receptors identified for toxin A and B, further studies are required to understand what region(s) of the toxins are binding to what type of receptors.

Upon receptor binding, the toxin is thought to be internalised into the endosome (Florin and Thelestam, 1983). TcdA and TcdB take the "short trip", which mean they arrange for the glucosyltransferase domain to escape from the endosome, instead of the retrograde transport through the Golgi apparatus ("long trip") (Genth *et al.*, 2008). In the intermediate part of the delivery domain, a (transmembrane) domain has been postulated to be involved in membrane translocation of the glucosyltransferase domain (Just and Gerhard, 2004). The pH drop in the acidified endosome is thought to induce a structural re-arrangement of the transmembrane domain allowing this domain to form a pore into the endosomal membrane (Giesemann *et al.*, 2006). Once the glucosyltransferase domain has passed the pore and reached the cytosol, it is proteolytically cleaved off from the rest of the protein in the presence of non-proteinaceous cofactors such as inositol phosphates (Egerer *et al.*, 2007; Figure 4). It is free to mono-glucosylate and, thereby, inactivate low molecular mass GTP-binding proteins of the Rho subfamily (avoiding the GDP-GTP exchange) (Herrmann *et al.*, 1998). The Rho subfamilies, which are more probably to be affected by these toxins, are: RhoA, Rac1 and Cdc42. This toxicity will compromise the actin cytoskeleton integrity, resulting rounding cells and cell death (Genth *et al.*, 2008).

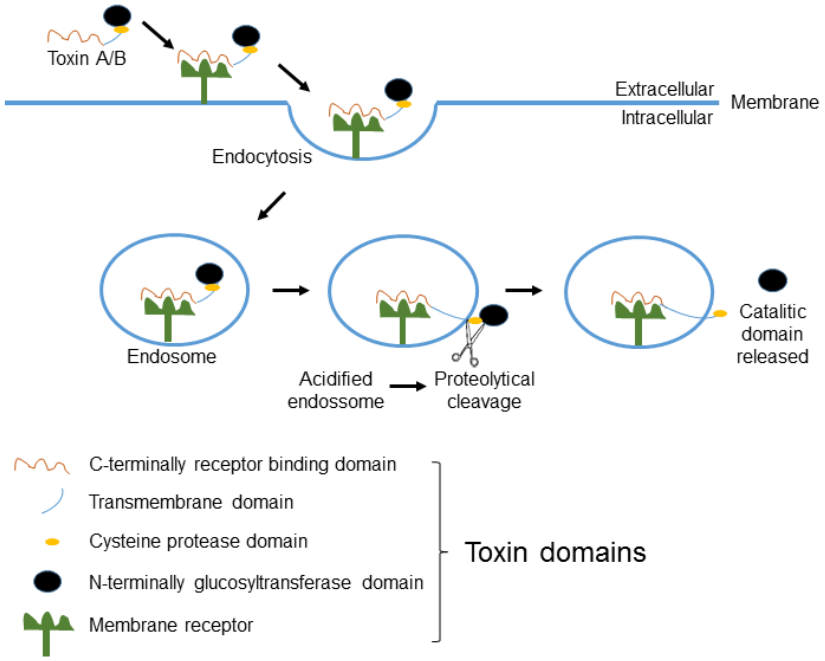

Figure 4 - Model of the uptake of *C. difficile* toxins. Toxins A and B bind to receptors on the surface of target cells and are endocytosed. Acidification of the toxins in endosomes exposes hydrophobic regions of the protein allowing their insertion into the membrane. At this point, the toxin forms a pore, and the N-terminal catalytic domain is translocated from an acidic endosomal compartment into the cytosol. The location of toxin processing is indicated by scissors. In the cytosol, the toxins are capable of glycosylating Rho subfamily proteins. The Figure is according to Rupnik *et al.*, 2009, with minor modifications.

In respect to their role in host–pathogen interactions, Rho proteins essentially participate in epithelial barrier functions and cell–cell contact, in immune cell migration, phagocytosis, cytokine production, wound repair, immune cell signalling, and superoxide anion production (Jank *et al.*, 2007). Rho proteins are regulated by a guanosine triphosphatase (GTPase) cycle and they are inactive in the guanosine diphosphate (GDP)-bound form. Activation occurs after GDP/GTP exchange, which is induced by guanine nucleotide exchange factors (GEFs). In the active form, the Rho proteins interact with numerous effectors and adaptors (Jank *et al.*, 2007).

Toxin-catalysed modification of Rho and Ras proteins have several functional consequences. Firstly, after glucosylation, Rho/Ras proteins are no longer able to interact with their effectors (Herrmann *et al.*, 1998; Sehr *et al.*, 1998). Secondly, glucosylation inhibits the activation of small GTPases by GEFs (Herrmann *et al.*, 1998; Sehr *et al.*, 1998). Finally, glucosylated Rho proteins are associated with the cell membrane and the membrane-cytosol cycle is blocked (Genth *et al.*, 1999). However, the most important structural consequence of glucosylation is probably inhibition of the change into the active conformation of the GTPase.

1.3.3. The holin-like protein TcdE

The *tcdE* open reading frame encodes a small, hydrophobic protein of 166 amino acids with a short hydrophilic stretch at the N-terminus, a series of charged residues at the C-terminus (Tan *et al.*, 2001) and is predicted to contain three transmembrane domains (Govind and Dupuy, 2012). These structural features and primary sequence similarities strongly suggest that TcdE is a member of the class I holins of which phage λ S protein is a member. Holins are small membrane proteins encoded by double-stranded DNA phages that are required for the lysis of host cells at a programmed time after completion of intracellular phage development (Wang *et al.*, 2000; Young *et al.*, 2000). They form disruptive lesions by oligomerization in the host cell plasma membrane to allow a prophage-encoded endolysin (a muralytic enzyme) to cross the membrane and attack the murein, resulting in cell lysis and release of phage particles (Wang *et al.*, 2000; Young *et al.*, 2000).

Two studies that support this idea are the overexpression of TcdE in *Escherichia coli*, causing cell death (Tan *et al.*, 2001) and the expression of TcdE from its own promoter

using a multicopy plasmid, which was lethal to *C. difficile* (Govind and Dupuy, 2012). However, a third study using a controlled expression vector to avoid *C. difficile* death, has shown that when high concentrations of the inducer were added (>50 ng/ml), the culture supernatant of the complemented *tcdE* mutant had a higher concentration of toxins than did the parent strain JIR8094 (Govind and Dupuy, 2012). Hence, under normal conditions, *C. difficile* presumably produces an amount of TcdE sufficient to form pores that allow release of toxin without causing cell lysis (Govind and Dupuy, 2012).

Until now, it is not known how these pores interact with toxins. If the toxins are secreted unfolded, possibly via translationally coupled secretion, only a narrow channel in the cytoplasmic membrane would be needed. Such a channel would not allow cytoplasmic protein leakage (Govind and Dupuy, 2012). On the other hand, if the toxins are secreted as fully folded proteins, a large membrane channel would be needed due to the volumes the large toxin proteins would occupy. Although TcdE has the intrinsic ability to form pores in the membrane that lead to permeability and cell death, as seen in *E. coli* (Tan *et al.*, 2001), it does not normally do so in *C. difficile* (Govind and Dupuy, 2012). If TcdE-dependent pores are formed in *C. difficile*, they should be tightly regulated by a mechanism that could include the toxins themselves. The toxins could, for instance, act as plugs to prevent loss of solutes or proteins from the cells through the TcdE pore. Such a model is consistent with the observation that a *tcdA tcdB* double mutant lysed more rapidly than the parental and PaLoc negative strains (Govind and Dupuy, 2012).

Finally, TcdE-dependent channels might be formed in association with other proteins that control the opening of the pore or TcdE could form a specific gated channel that only opens in the presence of TcdA/TcdB, without inducing cell lysis (Govind and Dupuy, 2012).

Another study showed that the inactivation of *tcdE* in the low-virulence strain 630Δ*erm*, did not significantly alter neither the kinetics of release nor the absolute level of secreted TcdA and TcdB (Olling *et al.*, 2012). Thus, the impact of TcdE in toxin secretion is still under debate.

1.4. Other PaLoc regulators

The spectrum of diseases caused by *C. difficile* is highly variable and depends on the level of toxin produced (Akerlund *et al.*, 2006). This supports the hypothesis that regulation of toxin synthesis is a critical determinant of *C. difficile* pathogenicity. Toxin synthesis increases as cells enter into stationary phase (Hundsberger *et al.*, 1997), and many environmental factors influence their production. In the presence of phosphotransferase system (PTS) sugars, such as glucose, and of certain aminoacids, like cysteine or proline, toxin production is inhibited (Dupuy and Sonenshein, 1998; Karlsson *et al.*, 2000). Environmental stresses, such as alteration of the redox potential, exposure to sub-inhibitory concentrations of antibiotics, high temperature, or limitation of biotin, also modulate toxin production (Onderdonk *et al.*, 1979; Yamakawa *et al.*, 1996; Karlsson *et al.*, 2003; Deneve *et al.*, 2009).

Several regulators are now implicated in toxins synthesis: CodY and Spo0A, two regulators that control pre- or post-exponential events, (Dineen *et al.*, 2007; Underwood *et al.*, 2009), CcpA, a glucose-dependent repression mediator (Antunes *et al.*, 2011) and SigH, a key element in the control of the transition from exponential to the stationary phase and of the initiation of sporulation (Saujet *et al.*, 2011). CodY is the first regulator encoded outside of the PaLoc that has been shown to participate in the regulation of toxin synthesis. Inactivation of the *C. difficile codY* gene resulted in derepression of all genes of the PaLoc during exponential and stationary growth phases, although this repression was not so pronounced in *tcdC* expression (Dineen *et al.*, 2007). Moreover, CodY binds to the *tcdR* promoter region but not to *tcdA* and *tcdB* promoters, suggesting that growth phase dependent regulation of *C. difficile* toxin synthesis is mediated by the effect of CodY on *tcdR* transcription (Dineen *et al.*, 2007). This binding was also enhanced in the presence of GTP and branched-chain amino acids, thus, regulation by CodY may provide a nutritional link to the pathogenicity of *C. difficile* (Dineen *et al.*, 2007).

Repression of toxin synthesis in the presence of glucose or other rapidly metabolizable carbon sources suggests that the toxin genes are subject to a form of catabolic repression (Dupuy and Sonenshein, 1998). In low G+C Gram-positive bacteria, carbon catabolite repression (CCR) is mediated by CcpA. To test this correlation, crude extracts of the parental strain were obtained from cells collected during stationary phase (14 h) and the total toxin levels were assayed by Vero cell cytotoxicity assays. In cells grown in the

presence of glucose, the cytotoxic activity was low as compared with that of cells grown without glucose. Moreover, using specific antibodies against TcdA, researchers also showed by Western blot that toxin A accumulation was strongly repressed in the presence of glucose (Antunes *et al.*, 2011). Moreover, the cytotoxic activity and the quantity of TcdA detected in crude extracts of the *ccpA* mutant grown in the absence or in presence of glucose were the same, which indicates that CcpA mediates glucose repression of toxin synthesis (Antunes *et al.*, 2011). Furthermore, the same study showed that the effect of CcpA is direct since this regulator interacts with the *tcdB* promoter region and the 5′ end of the *tcdA*-coding sequence (Antunes *et al.*, 2011).

Taking this into consideration, CodY and CcpA act by monitoring the nutrient sufficiency of the environment, directly repressing the PaLoc genes, and releasing this repression during stationary phase, when nutrient condition become limited (Dineen *et al.*, 2007; Antunes *et al.*, 2011).

Regarding Spo0A, this protein is conserved in all spore-forming bacteria, essential in the initiation of the developmental pathway of spore formation, and was also reported to be a PaLoc repressor (Zhao *et al.*, 2002; Underwood *et al.*, 2009). However, recent studies have failed to elucidate the role of Spo0A in TcdA and TcdB production by *C. difficile*, with conflicting data published to date (Underwood *et al.*, 2009; Deakin *et al.*, 2012; Rosenbusch *et al.*, 2012; Mackin *et al.*, 2013). In "hypervirulent" strains, as R20291, Spo0A acts as a negative regulator of TcdA and TcdB production (Deakin *et al.*, 2012). In contrast, Spo0A does not appear to regulate toxin production in the low-virulence strain 630Δ*erm* (Rosenbusch *et al*., 2012). Moreover, in other strains (as JGS6133), Spo0A appears to negatively regulate toxin production during early stationary phase, but has little effect on toxin expression during late stationary phase (Mackin *et al.*, 2013). These data suggest that Spo0A may differentially regulate toxin production in distinct *C. difficile* strain types. In any case, as no Spo0A boxes are present upstream of the *tcdA* and *tcdB* genes, an indirect effect of Spo0A on their transcription may happen via a still uncharacterized regulator (Underwood *et al.*, 2009).

Another study established a correlation between the PaLoc components and *sigH* expression in the stationary phase. *tcdR*, *tcdB* and *tcdA* showed increased transcription in the *sigH* mutant than in the 630Δ*erm* strain, while in the *sigH* complemented strain, the expression was restored to the level observed in 630Δ*erm* strain for all the three genes.

Therefore, the expression of these three genes is negatively controlled by σ^H (Saujet *et al.*, 2011). However, no σ^H consensus sequences are present in the PaLoc, suggesting an indirect effect of σ^H in the inhibition of the PaLoc transcription. Because the expression of *tcdC* was similar in the 630Δ*erm* strain and in the *sigH* mutant, authors suggested that the absence of modulation of *tcdC* transcription in the *sigH* mutant indicates that the σ^H-dependent control of *tcdA, tcdB,* and *tcdR* expression is not mediated by the regulation of TcdC synthesis (Saujet *et al.*, 2011). However, they could not exclude the possibility that σ^H may influence factors controlling TcdC stability and/or activity (Saujet *et al.*, 2011).

In conclusion, there are four negative regulators encoded outside the PaLoc that participate in the regulation of toxin production. These are some examples of the possible PaLoc regulators, which indicates us that the toxins production is a process that needs to be extremely well controlled, since these are the major virulence factors of *C. difficile*.

1.5. Genetic tools and single-cell analysis of the PaLoc expression

Although a very important pathogen, only recently a solid platform of genetic and cell biology tools was developed for *C. difficile.* Studies to understand in more detail *C. difficile* colonization, virulence and pathogenesis are now possible. First, directed mutants could only be made using insertional mutagens, reliant either on replication deficient (Liyanage *et al.*, 2001) or defective (O'Connor *et al.*, 2006; Dineen *et al.*, 2007) plasmids, or on the deployment of the ClosTron and group II intron re-targeting (Heap *et al.*, 2007; Heap *et al.*, 2010). Recently, the cytosine deaminase gene (*codA*) of *E. coli* was developed as a negative/counter selection marker for *C. difficile*, which enabled precise manipulation of the *C. difficile* chromosome for the first time (Cartman *et al.*, 2012). In parallel, a second method (Allele-Coupled Exchange, ACE) has been formulated that allows the rapid insertion of heterologous DNA, of any size or complexity, into the genome (Heap *et al.*, 2012). Because the ACE mutagenesis system allows a specific in-frame deletion, which reduces the polar effects, this was the chosen system for this work. In other hand, the autofluorescence proteins (AFP's) that have enable noninvasive imaging in living cells of reporter gene expression and therefore have become indispensible tools in cell and development biology, cannot be applied in strict anaerobes like *C. difficile*. Recently, our laboratory has implemented a system based on a mutant form of the human DNA repair enzyme O6-alkylguanine-DNA alkyltransferase

(SNAP^{Cd}-*tag*) (Pereira *et al.*, 2013) to examine gene expression in single cells of *C. difficile* (Figure 5). The SNAP^{Cd}-*tag* reacts with benzyl purine or pyrimidine substrates that can be coupled to different fluorescent molecules (TMR-star which is commercially available, Figure 5).

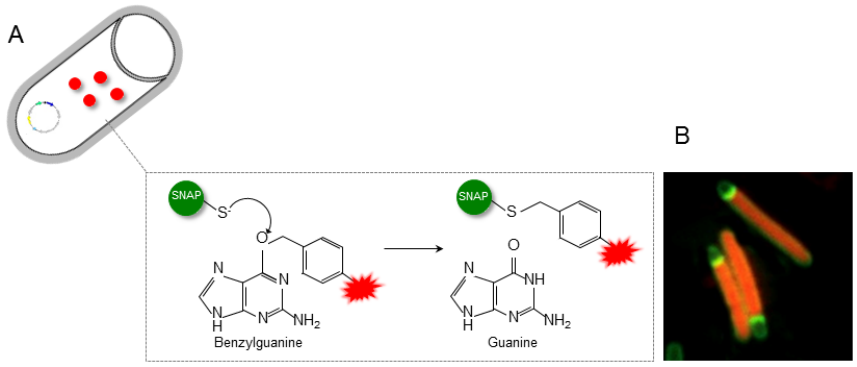

Figure 5 - The SNAP^{Cd} technology extended to *C. difficile*. A: Schematic representation of SNAP^{Cd} labelling. *C. difficile* cells carry a replicative plasmid where the *SNAP^{Cd}* sequence is under the control or fused to a gene of interest. These cells are cultivated under appropriate conditions that allow production of the SNAP^{Cd} protein, time at which a cell permeable label (red) should be added. The permeable label enters into the cell, where a covalent modification occurs, allowing labelling and visualization of the SNAP^{Cd} protein by fluorescence. B: Microscopy analysis of *C. difficile* cells producing SNAP^{Cd} visualized by the red color after labelling with the TMR-Star cell-permeable SNAP^{Cd} substrate (Pereira *et al.*, 2013).

Although a wealth of literature has addressed the process of toxinogenesis in *C. difficile*, expression of the *tcdA* and *tcdB* genes, and indeed of the other three PaLoc genes, was never studied at the single-cell level. This kind of study is very important given the increase evidence that exist cell-to-cell differences at the gene expression level in bacterial populations. Such gene expression heterogeneity determines the fate of individual cell and can also ultimate the fate of the population as a whole.

In preliminary work made in the laboratory we have fused the *tcdR, tcdB, tcdE, tcdA* and *tcdC* promoters (all the regulatory regions of the PaLoc genes) to the SNAP^{Cd}-*tag* and assessed gene expression in a medium that support toxin production in the standard laboratory strain 630Δ*erm* (Figure 6). Two cellular populations expressing *tcdR* during stationary phase were observed, a smaller one consisted of cells without signs of asymmetric division; a larger one consisted of sporulating cells in which, strikingly, *tcdR* is expressed in the forespore (Figure 6B). As expected, fluorescence was not detected during exponential growth (data not shown). These results already show that the PaLoc expression is spatially and temporally regulated. Since we found *tcdR* to be expressed in the forespore, we therefore anticipated accumulation of the toxin in the developing spore.

tcdB and *tcdE* have similar patterns of expression to *tcdR*. *tcdA* is also expressed in two populations during stationary phase, in cells without signs of asymmetric division and also in sporulating cells, both in the mother cell and in the forespore (Figure 6).

In contrast, *tcdC* expression was detected during exponential growth (data not shown). During stationary phase, *tcdC* is also expressed in either cells without signs of asymmetric division or in the mother cell during sporulation. However, expression of *tcdC* was never detected in the forespore.

Given these results, it is pertinent to go depth in the study of the cell population dynamics with respect to the circuits governing toxinogenesis and sporogenesis.

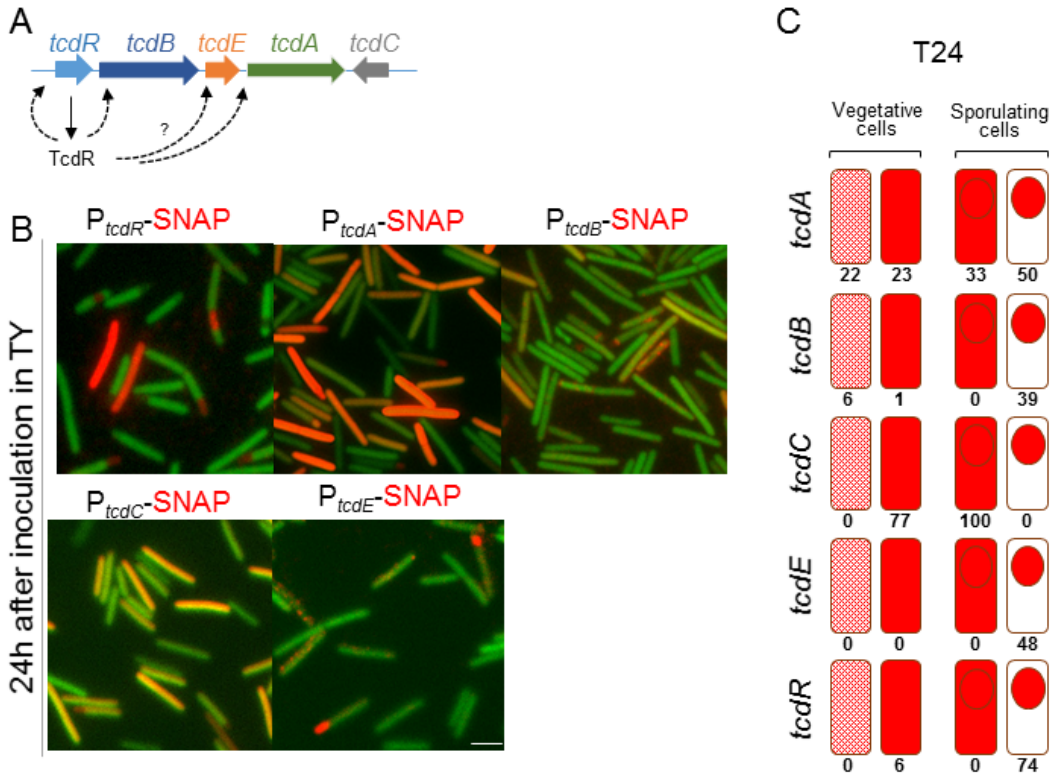

Figure 6 - Fluorescence microscopy using SNAP^{Cd}-*tag* fused to different promoters of the PaLoc components (*tcdR, tcdB, tcdE, tcdA* and *tcdC*). A: Regulatory interactions in the Pathogenicity Locus. TcdR is thought to be auto-regulatory; TcdR also activates transcription from the indicated PaLoc promoters; B: Cells were incubated 24h in TY medium and observed by fluorescence microscopy. The green color corresponds to *C. difficile* autofluorescence while the red one corresponds to the reaction of the SNAP^{Cd} reporter with the TMR-Star substrate. *tcdR* expression is mainly detected in the forespore, as is that of *tcdB*. The expression of *tcdA* appears mostly in vegetative and mother cells but also in some forespores. *tcdC* expression seems to be excluded from the forespore. Finally, *tcdE* was mainly expressed in the forespore. Scale bar: 1µm; C: Percentages of each of the following cell classes: vegetative cells with little expression (light red) and high expression (red) and sporangia with whole cell expression or only in the forespore.

1.6. Objectives of the work

The preliminary results described above show that sporulation and toxinogenesis are interconnected, with expression of the PaLoc genes during sporulation. To increase our knowledge on the relationship between toxinogenesis and sporogenesis, we focused our attention on the regulation of *tcdR* expression and on the role of *tcdE* on TcdA secretion and localization. Our specific aims were:

1. To construct a *tcdR* mutant, and to study the impact of this mutation on *tcdA* and *tcdR* expression, on growth and on sporulation. Since *tcdR* expression was detected in the forespore, we followed this clue to study the relationship between sporulation and toxin production. Furthermore, this mutant was crucial to understand the relevance of the *tcdR* positive feedback and to confirm *tcdA* regulation by TcdR.
2. To analyze the accumulation and localization of TcdA in the mature spore, since expression of *tcdA* was detected in both the mother cells and in the forespore.
3. To construct a *tcdE* mutant, and to study the impact of the mutation on toxin secretion and on the localization of the toxin in the mature spore.

2. Material and methods

2.1. Microbiological techniques

2.1.1. Bacterial strains and growth conditions

Escherichia coli strain DH5α was used as a host for molecular cloning and for plasmid propagation (Appendix 1); *E. coli* strain HB101 was used for conjugation of plasmids into *C. difficile* due to the presence of the conjugational plasmid RP4. Luria Bertani (LB) medium (1% tryptone, 0.5% yeast extract, 0.5% NaCl, pH 7.0) was routinely used for growth and maintenance of *E. coli*. When necessary, agar (Agar nº2 bacteriological, from LAB M) was added to a final concentration of 1.6%. When appropriate, ampicillin (100 µg/mL) or chloramphenicol (20 µg/mL) was added to the culture medium.

All the strains of *C. difficile* used in this work are congenic with 630Δ*erm* (Hussain *et al.*, 2005), the reference strain in the field, and are listed in Appendix 2. Strain 630Δ*erm* is hereinafter referred to as the wild type (WT) for simplicity and belongs to the ribotype 012, which is not classified as "hypervirulent". All strains were stored at -80ºC in 20% glycerol. *C. difficile* strains were routinely grown anaerobically (5% H_2, 15% CO_2, 80% N_2) at 37ºC in brain heart infusion (BHI; from Oxoid) or in BHI supplemented with 0.1% L-cysteine and 5 mg/ml yeast extract (BHIS). Bacto agar (from BD) was normally used at a final concentration of 1.6%. A *C. difficile* minimal medium (CDMM; Karasawa *et al.*, 1995) solidified with 1.5% agar (from BD) was required for the ACE mutagenesis (see below; Appendix 3). CDMM was supplemented with 5-fluoroorotic acid (2 mg/ml) and uracil (5 µg/ml) when appropriate. For some experiments, *C. difficile* was grown in Tryptone Yeast Extract medium (TY: 3% bacto tryptone, 2% bacto yeast extract). When necessary, cefoxitin (25 µg/ml) and thiamphenicol (15 µg/ml) were added to *C. difficile* cultures. For *tcdE* complementation anhydrotetracycline (ATc) was used at a concentration of 20 ng/ml.

Sporulation assays were performed in Sporulation Medium (SM): 9% bacto tryptone, 0.5% bacto peptone, 1% $(NH_4)_2SO_4$ and 0.15% Tris base, pH 7.4 (Wilson *et al.*, 1982). The pre-inoculumn was inoculated in SM medium (1:200 dilution) and, after 24, 48 and 72 hours the sporulation efficiency was analysed. Serial dilutions were performed (up to

10^{-6}) and three spots (20 µl) of each of the 10^{-6}, 10^{-5}, 10^{-4} and 10^{-3} dilutions were spotted onto BHI plates containing 0.1% taurocholate acid sodium salt (from Roth) to induce spore germination. The 10^{-1}, 10^{-2}, 10^{-3} and 10^{-4} diluted cultures were removed from the chamber and incubated 30 minutes at 60°C to kill vegetative cells. Finally, these were introduced again inside the chamber and three spots of 20 µl were spotted onto a BHI plate containing 0.1% taurocholate. All plates were incubated overnight under anaerobic conditions. The colonies counting was concluded after 24h of the plates inoculation and the sporulation efficiency was calculated according to the following formula:

$$\text{cfu/ml} = \text{number of colonies} \times \frac{1}{\text{Dilution}} \times \frac{1}{\text{Volume}}$$

Dilution – Dilution factor (*e. g.*, 10^{-2}, 10^{-3}).

Volume – Plated volume in ml.

For spore production, *C. difficile* was grown in BHI. An overnight culture was added to BHI liquid medium in a T-flask with a final dilution of 1:100. Cultures were incubated anaerobically in the horizontal for 7 days at 37ºC. Cells were collected by centrifugation at 4700 x *g*, resuspended in cold water and stored over 48h at 4ºC, for lysis of mother cells and release of the spores. The suspension was centrifuged again for 10 minutes at 4700 x *g*, 4ºC and the sediment was suspended in 1 ml of 1x PBS (137 mM NaCl, 2.7 mM KCl, 4.3 mM Na_2HPO_4, 1.4 mM KH_2PO_4, pH 7.6) 0.1% tween 20 (PBS-T). This suspension was applied on top of 25 ml of a 42% Gastrografin solution (from Bayer) and centrifuged for 20 minutes at 4700 x *g*, 4ºC. The supernatant was then aspirated using a vacuum apparatus and the sediment suspended again in 1 ml of PBS-T. Two more washes in PBS-T were performed (to remove traces of Gastrografin) at 4700 x *g* during 3 minutes at room temperature. Lastly, the sediment was washed two times in water and, finally, suspended in 500 µl of water.

2.1.2. Bacterial growth

Cultures were incubated under anaerobic conditions and growth was followed by measuring the optical density at 600 nm (OD_{600}) at hourly intervals. The growth rate was calculated from the slope of the part of the curve that corresponds to the exponential growth phase, while the generation time was determined according to the following equation: generation time = ln(2)/growth rate.

2.2. Biochemical techniques

2.2.1. Spore fractionation

The volume of a purified spore suspension used in fractionation experiments was determined by measure of spore suspension OD_{580}, previously diluted 1:200 in bi-distiled water (ddH_2O), and using the following formula:

$$\text{Volume of suspension (µl)} = (3600/OD_{580}) \times 200$$

The spores were resuspended in 50 µl of 2X decoating buffer (10% glycerol, 4% SDS, 10% β-mercaptoethanol, 1 mM DTT, 250 mM Tris, pH 6.8). Samples were boiled for 5 minutes and centrifuged 2 minutes at 16200 x *g*. Finally, supernatants were collected to a new tube and 2 µl of 1% bromophenol blue were added. 25 µl of the samples were applied on a 12.5% SDS-PAGE gel (12.5% resolving gel: 41% distilled water, 25.4% 4x lower Tris buffer, 12.6% bis-acrylamide, 0.1% SDS, 0.1% ammonium peroxydisulphate, 0.05% tetramethylethylenediamine, these last two induced polymerization; 4.5% stacking gel: 61.2% distilled water, 25.5% 4x upper Tris buffer, 10.2% bis-acrylamide, 0.1% SDS, 0.1% ammonium peroxydisulphate, 0.1% tetramethylethylenediamine).

The sediments resulting from the spore decoating step were washed twice in PBS-T. Sediments were suspended in 100 µl of PBS-T and divided in two tubes. These were centrifuged 3 minutes at 4700 x *g* and one of the two sediments was suspended in 25 µl of 50 mM Tris HCl, pH 8.0 with 2 mg/ml lysozyme, while the other was suspended in 25 µl of 50 mM Tris HCl, pH 8.0. Samples were incubated at 37°C for 2 hours and, after this time, 25 µl of loading buffer 2X (0.125 mM Tris-HCl, 5% β-mercaptoethanol, 2% SDS, 0.025% bromophenol blue, 0.5% mM DTT, 5% glycerol, pH 6.8) were added. For each of the samples, 50 µl were resolved by SDS-PAGE gel (12.5% gels). The Precision Plus Protein™ All Blue Ladder (from BioRad) was used in each run.

The resulting gel was incubated 1 hour in the coomassie solution (0.5 g/ml coomassie Brilliant Blue R-250, 80% absolut ethanol, 20% acetic acid) and then, incubated in destaining solution (30% absolut ethanol, 10% acetic acid) overnight with agitation at room temperature. In the next day, the gel was incubated with new destaining solution until the background was clear.

2.2.2. Western blot

Proteins were electrophoretically transferred from SDS-PAGE gel to nitrocellulose membranes (Supported Nitrocellulose, 0.45 µm; from BioRad) at 100 V for 90 minutes using transfer buffer (14.4 g/L glycine, 3.02 g/L Tris base, 10% ETOH). The membrane was incubated in 20 ml of blocking solution (5% milk in PBS-T) for 1 hour with agitation. Next, the blocking solution was removed and the antibody solution was added in 10 ml of PBS-T with 0.5% milk [An anti-TcdA antibody (from Santa Cruz Biotechnology) was used at a dilution of 1:5000; an anti-CotD antibody (Permpoonpattana *et al.*, 2011) was used at a dilution of 1:1000 and an anti-CotA antibody (Permpoonpattana *et al.*, 2011) was used at a dilution of 1:3000]. The membrane was incubated overnight with the antibody solution at 4°C without agitation. The antibody solution was then discarded and the membrane was washed 3 times in PBS-T (10 minutes each wash). The secondary antibody (mouse peroxidase-conjugated secondary antibody from Sigma) was then added in 10 ml of PBS-T with 0.5% milk at a dilution of 1:2000. The membrane was incubated 30 minutes at room temperature with agitation. Finally, the membrane was washed 3 more times in PBS-T (10 minutes each) and the protein was detected using the detection solution ("SuperSignal West Pico Chemiluminescent" from Thermo Scientific) in the dark.

For reprobing, membranes were incubated in 20 ml of a stripping solution (6.25% Tris-HCl pH 6.8, 2% SDS, 0.7% 2-mercaptoethanol) for 30 minutes at 50ºC (with agitation every 10 minutes). Then, the membrane was washed in distilled running water and incubated in blocking solution. The remaining of the protocol is the same as described above.

2.2.3. Dot blot

This technique represents a simplification of the western blot method. In a dot blot, the biomolecules are not separated by electrophoresis as the western blot requires. Instead, a mixture containing the molecule which we want to detect is applied directly on a membrane as a dot. This is then followed by antibody detection (see above 2.2.2).

C. difficile cultures were centrifuged and two fractions were obtained, the sediment and the supernatant. 10 ml of the supernatant was concentrated up to 1 ml in an Amicon Ultra-4 Centrifugal Filter Unit with Ultracel-50 membrane and 200 µl of the concentrated

solution were analysed by dot blot, except when the total amount of proteins were normalized (see 2.2.4), in this case, different volumes of each sample were used. The sediment resulting from the centrifugation was suspended in 1 ml of French press buffer (10 mM Tris pH 8.0, 10 mM $MgCl_2$, 0.5 mM EDTA, 0.2 mM NaCl, 10% glycerol, 1 mM PMSF) and cells were lysed at 900 psi. 1 µl of DNAse was added to this extract which was then clarified by centrifugation for 10 minutes at 16200 x *g*, 4ºC. 20 µl of the supernatant were analysed by dot blot, except when the total amount of proteins were normalized (see 2.2.4).

2.2.4. Bradford protein assay

This is a spectroscopic analytical procedure used to measure the protein concentration in a solution. The protein assay-dye (from BioRad) was diluted 5x in ddH_2O. For the reference, 200 µl of this diluted solution were added to 800 µl of ddH_2O. In order to measure the protein concentration, 10 µl of each sample were added to 200 µl of the diluted Bradford solution and 790 µl of ddH_2O. The absorbance (*A*) of the mixture was measured at 595 nm and the protein concentration was calculated according to the following formula:

$$(\mu g/\mu l)=\frac{\left(\frac{A_{595}}{0.0656}\right)}{10}$$

2.3. Genetics and molecular biology techniques

2.3.1. Molecular cloning

DNA fragments for cloning were generated by the polymerase chain reaction (PCR) using the high fidelity Phusion DNA polymerase (from Thermo Fisher Scientific). All oligonucleotide primers used in this work are listed in Appendix 4. PCR products were purified and concentrated using the DNA Clean and Concentrator^{TM} – 5 kit (from Zymo research). General cloning methodologies were as previously described (Sambrook and Green, 2012). All DNA restriction and modification enzymes were obtained from Thermo Fisher Scientific and used according to the manufacturer's guidelines. All the plasmids

used and constructed during this work are listed in Appendix 5. The sequence of all newly constructed plasmids was verified by DNA sequencing.

2.3.2. Gel electrophoresis of nucleic acids

In order to verify the presence of specific DNA fragments, samples were subjected to 1% agarose gels in TAE 1X (50X: 242 g/L Tris base, 5.71% glacial acetic acid, 10% 0.5 M EDTA, pH 8.0) buffer. Before application in the gel, orange G loading buffer (2.5% ficoll-400, 11 mM EDTA, 3.3 mM Tris-HCl, 0.017% SDS, 0.15% orange G, pH 8.0) was added to the sample. These gels run in the presence of ethidium bromide [0.001% (v/v)] at 110 Volts. The DNA was visualized using UV light (205 nm). The size of the fragments was measured by comparison with commercial molecular weight marker 1 Kilo base pair (Kb) Plus DNA Ladder (from Invitrogen).

2.3.3. Preparation of *E. coli* competent cells and transformation

In order to cells have the ability to uptake extracellular DNA from the environment, they need to be competent. However, when it does not occur naturally in some bacteria, as *E. coli*, it can be induced. To achieve that, fresh LB medium (100 ml) was inoculated with 200 µl of an overnight *E. coli* culture and incubated at 37°C to an OD_{550nm} ~ 0.3-0.4. This culture was placed on ice for 15 minutes and centrifuged at 900 x *g* for 15 minutes at 4°C. Then, the supernatant was removed and the sediment was resuspended in ice-cold RF1 buffer, pH 5.8 (12 mg/ml RbCl, 9.9 mg/ml $MnCl_2$, 1.5 mg/ml $CaCl_2$, 11% glycerol, 3% KAc 1M pH 7.46) by pipetting gently up and down (30 ml per 100 ml of culture). After a 15 minutes incubation on ice, the tube was, again, centrifuged at 900 x *g* for 15 minutes at 4°C and the supernatant was removed. Then, the sediment was resuspended in 8 ml of ice-cold RF2 buffer, pH 6.8. (1.2 mg/ml RbCl, 8.3 mg/ml $CaCl_2$, 10% glycerol, 2% MOPS 0.5 M, pH 6.8).

The transformation process happens when a cell incorporates exogenous genetic material from the surroundings. First, cells need to contact with the plasmid, therefore, 10 µl of the ligation mixture were added to 200 µl of competent *E. coli* cells followed by a 40 minutes incubation on ice. A thermal shock was performed during 90 seconds at 42°C and then 2 minutes on ice.

After cells recover in 1 ml of LB at 37°C for two hours, the tube was centrifuged 5 minutes at 3500 x *g*. 1 ml of the supernatant was discarded and the sediment was resuspended in the remaining volume. All of this content was plated in LA with the appropriate antibiotics and incubated overnight at 37°C.

2.3.4. Extraction of plasmid DNA

In order to detect the transformant colony carrying the plasmid of interest, minipreps were performed to extract the plasmid DNA. The verification of the insert was done using restriction enzymes that digest not only the vector but also the insert.

An isolated colony resulting from *E. coli* DH5α transformation was incubated overnight in 5 ml of LB with the appropriate antibiotic. 2 ml of this culture were centrifuged 5 minutes at 16200 x *g* and the sediment was resuspended in 394 µl of a solution containing 360 µl of STET buffer (8% sucrose, 0.5% Triton X-100 (v/v), 50 mM EDTA, 10 mM Tris-HCl, pH 8.0), 24 µl of lysozyme (10 mg/ml) and 10 µl of RNAse (10 mg/ml). The tube was incubated at 37ºC for 30 minutes and after that, it was boiled for 1 minute. Then, it was centrifuged at 16200 x *g* for 5 minutes and the sediment was removed with a loop. Isopropanol was added to the remaining content at a final concentration of 70% (v/v) and the tube was, again, centrifuged at 16200 x *g* for 45 minutes at 4ºC. Finally, the supernatant was carefully decanted, the sediment was air dried and 20 µl of ddH_2O were added to suspend the sediment.

When the goal was to extract the plasmid to transform HB101 cells and to confirm the DNA sequence by sequencing, the "ZR-plasmid Minipreps kit classic" (from Zymo research) was used, since the efficiency of this technique is much higher than the one presented above. This method is based on the alkaline lysis of cells and adsorption of DNA to a silica matrix immobilized in a column, which is then eluted.

2.3.5. *C. difficile* conjugation

The conjugation process is another DNA transference method that requires direct cell-to-cell contact and a bridge-like connection between two cells. Using *E. coli* HB101 (pRP4) strain as a donor, the plasmids were transferred by conjugation into *C. difficile* strains as described previously (Purdy *et al.*, 2002). A single colony of *E. coli* HB101 with the plasmid of interest was inoculated in 5 ml of LB with the appropriate antibiotics

and incubated at 37ºC with agitation, overnight. Also, a single colony of *C. difficile* 630Δ*erm*Δ*pyrE* was inoculated in 10 ml of BHIS and incubated overnight (O/N) at 37ºC under anaerobic conditions. In the next day, 1 ml of the *E. coli* culture was centrifuged at 3000 x *g* for two minutes and the supernatant was discarded. The sediment was carefully washed in 1 ml of LB. *E. coli* cells were resuspended in 300 µl of *C. difficile* culture and the conjugative mixture was pipetted in 25 µl spots in a BHIS plate. This plate was not inverted and it was incubated under anaerobic conditions O/N. In the following day, cells were carefully scraped with a loop on the surface of the BHIS plate. This content was resuspended in 1 ml of BHIS and 150 µl of the mixture was plated in four BHIS plates supplemented with cefoxitin and thiamphenicol to select for strains that successfully received the plasmid. The cefoxitin will function as a selection of *C. difficile* against *E. coli*, while the thiamphenicol will select only cells that have the plasmid. The 400 µl leftovers were used to perform a 1:5 dilution and 150 µl of the diluted mixture were plated in four BHIS plates. Plates were incubated O/N at 37ºC under anaerobic conditions.

2.3.6. Allele-Coupled Exchange (ACE) mutagenesis

In ACE mutagenesis, a specific plasmid originated from pMTL-YN3 containing a truncated gene and the flanking regions (to allow recombination), is expected to integrate in the chromosome and replace the wild type gene by a truncated version of it. One of the requirements for this mutagenesis process is the prior inactivation of a gene which will allow a positive and a negative selection (Ng *et al.*, 2013). In this case, the gene is the *pyrE* which encodes an orotate phosphoribosyltransferase, an enzyme involved in *de novo* pyrimidine biosynthesis. This gene is given *in trans* in the plasmid originated from pMTL-YN3 (Ng *et al.*, 2013; Figure 7) that is used for the mutagenesis. It works as a positive/negative selection marker as it is essential in the absence of exogenous pyrimidines and it also renders 5-fluoroorotic acid (FOA) toxic to cells (Ng *et al.*, 2013). Toxicity occurs via a series of steps which result in misincorporation of fluorinated nucleotides (5-fluoruracil) into DNA and RNA and hence, cause cell death (Ng *et al.*, 2013).

Crucially, having created the interested mutants, a specific ACE-vector (pMTL-YN1; Appendix 5) was used to restore the chromosomal *pyrE* allele back to wild-type, allowing the specific in-frame deletion mutant to be characterised in a clean, wild-type background.

Also, a variant of the same vector (pMTL-YN1C; Appendix 5) is used to deliver the wild-type allele of the gene under study, allowing complementation studies.

An important characteristic is that the plasmids used in ACE mutagenesis are "pseudo-suicide" vectors, then, they should easily integrate in the chromossome (Cartman *et al.*, 2010, Cartman *et al.*, 2012).

The first conjugant colonies (see above section 2.3.5) that had the plasmid containing the in-frame deletion of the gene under study, started to appear after two or three days and the isolated ones were streaked into BHIS supplemented with cefoxitin and thiamphenicol. This step was repeated one more time to select for the single cross-over, which means that the plasmid was integrated in the chromosome. After 2 to 3 days, the larger colonies were ready for the single cross-over verification. First, a loop was necessary to collect the isolated colony and inoculate into a new BHIS plate supplemented with cefoxitin and thiamphenicol, also, the same loop was used to resuspend in 5% chelex resin (Sigma-Aldrich). After the genomic DNA extraction (see below Chelex protocol in 2.3.7), the single cross–over was verified by PCR. The positive clone was then transferred to *C. difficile* minimal medium supplemented with FOA (2 mg/ml) and uracil (5 µg/ml). Colonies which grew in this medium were rounder and yellow than the usual and they took about 2/3 days to show up. The ones that were able to grow were tested for the plasmid excision by PCR which mean that the second single cross-over excised the plasmid with the *pyrE* gene and because of that, cells were resistant to the FOA. The positive clones were finally tested in BHIS supplemented with cefoxitin and thiamphenicol to exclude the presence of the plasmid (which have the thiamphenicol resistance mark) in the mutant strain.

At this point, a strain with deletion for the gene under study in a background Δ*pyrE* was constructed. To revert the *pyrE*$^{-}$ background, the strain was conjugated with *E. coli* HB101 (pRP4) carrying pMTL-YN1 (containing the *pyrE* gene; Ng *et al.*, 2013) and the conjugant colonies were then transferred into *C. difficile* minimal medium. The ones which grew in this medium, were analysed by PCR to confirm the *pyrE* reversion. The positive clones were finally tested in BHIS supplemented with cefoxitin and thiamphenicol to exclude the presence of the plasmid (which have the thiamphenicol resistance mark) in the mutant strain. To discard polar effects, trans-complementation analysis was conducted. Using *E. coli* HB101 (pRP4) strain as a donor, the

complementation plasmid originated from pMTL-YN1C (containing the WT gene under study in the *pyrE* locus) was transferred by conjugation into *C. difficile* 630Δ*erm*Δ*pyrE*Δ*tcdR/E* carrying the mutation. Conjugant colonies were transferred into *C. difficile* minimal medium and the ones that grew were analysed by PCR to confirm the presence of a copy of the interest gene at the *pyrE* locus. The positive clones were finally tested in BHIS supplemented with cefoxitin and thiamphenicol to exclude the presence of the plasmid (which bears the thiamphenicol resistance mark) in the mutant strain.

2.3.7. Genomic DNA extraction

C. difficile genomic DNA was extracted using the chelex (Sigma-Aldrich) resin that binds cellular polar components while the RNA and DNA remain in water solution.

A single colony was resuspended in 100 µl of 5% chelex resin. Then, cells were subjected to a heat shock at 95ºC for 10 minutes followed by a centrifugation at 10000 x *g* for 1 minute. Finally, 50 µl of the supernatant were collected and 1 µl was directly used for PCR.

2.4. Cell Biology

2.4.1. Fluorescence microscopy and image analysis

For $SNAP^{Cd}$ labelling, *C. difficile* was grown in TY for 24 hours. After this period, 200 µl of the culture were added to 1 µl of TMR (50 µM) to a final concentration of 250 nM and the mixture incubated for 30 min in the dark. Following labelling, the cells were removed from the anaerobic chamber and collected by centrifugation (3500 x *g* for 2 minutes at room temperature), washed 3 times in 1 ml of 1x PBS and, finally, resuspended in 10 µl of 1x PBS. Cells (4 µl) were mounted on a 1.7% agarose coated glass slide and observed on a Leica DM6000B microscope equipped with a phase contrast Uplan F1 100x objective and a CCD $Ixon^{EM}$ camera (from Andor Technologies; Serrano *et al.*, 2011). The images were taken with exposition time of 50 ms for bright field and 1000-3000 ms for TMR. Images were acquired and analysed using the Metamorph software suite version 5.8 (from Universal Imaging), and adjusted and cropped using Photoshop CS5. For quantification of the $SNAP^{Cd}$ signal resulting from the transcriptional fusions, 6x6 pixel regions were defined in the desired cell and the average pixel intensity was

calculated by the Metamorph software, and corrected by subtracting the average pixel intensity of the background.

3. Results

3.1. Construction and *in trans* complementation of an in-frame deletion mutant of *tcdR*

TcdR is an RNA polymerase sigma factor that serves as the main positive regulator of expression of the PaLoc genes, which is hence under positive auto-regulation (Mani *et al.*, 2001; 2002). Although the regulation of the PaLoc by TcdR has been studied *in vitro*, few studies have addressed the impact of a *tcdR* mutation on expression of the PaLoc during growth of *C. difficile* (Mckee *et al.*, 2013) and none at the single cell level. We first constructed a strain carrying an in-frame deletion of *tcdR* to understand how the absence of the protein would have an impact on the expression of the PaLoc genes and, since *tcdR* is expressed in the forespore (Figure 6), on sporulation.

The ACE methodology (Ng *et al.*, 2013) was used to inactivate the *tcdR* gene. An allele exchange cassette was assembled composed of a left-hand homology arm (LHA) and a right-hand homology arm (RHA) relative to *tcdR*. The LHA (645 bp) was amplified by PCR using primers *tcdR*-AscI-Fw and *tcdR*-SOE-Rev (bases 785966 to 786598 on the forward strand of the *C. difficile* 630Δ*erm* genome; Appendix 4). The RHA (555 bp, which includes the first 184 bp of *tcdB*) was amplified by PCR using primers *tcdR*-SOE-Fw and *tcdR*-SbfI-Rev (bases 787055 to 787576 on the forward strand of the *C. difficile* 630Δ*erm* genome; Appendix 4). The two fragments were joined by splicing by overlap extension (SOE) PCR and cloned between the AscI and SbfI sites of pMTL-YN3 (Ng *et al.*, 2013) to produce pSR3 (Appendix 5). The fusion of the LHA with the RHA creates an in-frame deletion removing codons 27 to 178 of *tcdR* gene.

pSR3 was introduced in *C. difficile* 630Δ*erm*Δ*pyrE* (Appendix 2) by conjugation. The transconjugants obtained were restreaked two times in BHIS with thiamphenicol and cefoxitin to select for the single crossover. Large colonies were tested for pure single crossovers clones by PCR using two pairs of primers (Figure 7): pair 1 *tcdR*-vef-Fw (P3) and YN3-vef-Fw (P2), and pair 2 *tcdR*-vef-Rev (P4) and YN3-vef-Rev (P1). Depending which homology arm undergoes recombination, the PCR's from the single crossovers will result with pair 1 in 1665 bp and pair 2 in 2014 bp fragments, or with pair 1 in 2121 bp and pair 2 in 1558 bp fragments (Figure 7A). Two colonies were shown by PCR to be

pure single crossovers (colonies 6 and 9; Figure 7B); colony 9 was selected to proceed with the mutagenesis.

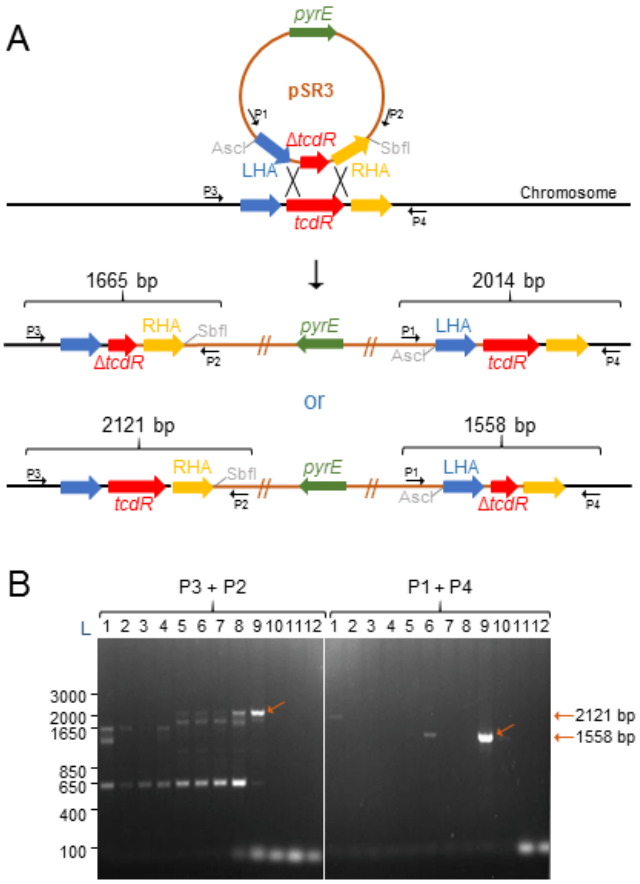

Figure 7 - ACE mutagenesis of the *tcdR* gene in the 630Δ*erm*Δ*pyrE* strain. A: In this simplified figure, pSR3 is composed by a left homology arm (LHA), the truncated gene previously amplified by SOE-PCR (Δ*tcdR*), a right homology arm (RHA) and the *pyrE* gene. These left and right homology arms are chromosome homology regions that will allow recombination and plasmid integration. This plasmid can integrate in two different ways which can be distinguish using P3 and P2 primers in a PCR reaction and P1 and P4 in another; B: Single cross-over analysis for *tcdR* mutagenesis. P3: *tcdR*-vef-Fw; P2: YN3-vef-Fw; P1: YN3-vef-Rev; P4: *tcdR*-vef-Rev. 1 to 12: tested clones. L: 1 Kb Plus DNA ladder. These results show that there are two clones (6 and 9) that have the integrated pSR3. Regarding figure A, both clones integrated the plasmid as shown in the second option, since they presented PCR products with 2121 bp and 1558 bp. Clone 9 was selected for further experiments.

Next, single colonies were re-streaked onto minimal medium supplemented with FOA and uracil to select for cells in which the integrated plasmid had excised. Depending which homology arm undergoes recombination, plasmid excision can result in either the desired double crossover mutant, or a wild type cell (Figure 8). The isolated FOA resistant colonies were then screened by PCR using primers *tcdR*-vef-Fw and *tcdR*-vef-Rev that anneal to the upstream and the downstream sequence of *tcdR*, respectively (Figure 8A). Of the 18 colonies screened, 11 yielded the expected 1901 bp DNA fragment, indicative

of an in-frame deletion (Figure 8B). The other colonies yielded a 2357 bp DNA fragment, consistent with the presence of a wild-type copy of the gene (Figure 8B). Colony 1 was chosen for the further studies (630Δ*erm*Δ*pyrE*Δ*tcdR*; Appendix 2). Colony 5 seemed to have both fragments, which probably mean that two colonies, instead of one, were used in the genomic DNA extraction, resulting in a mixed culture.

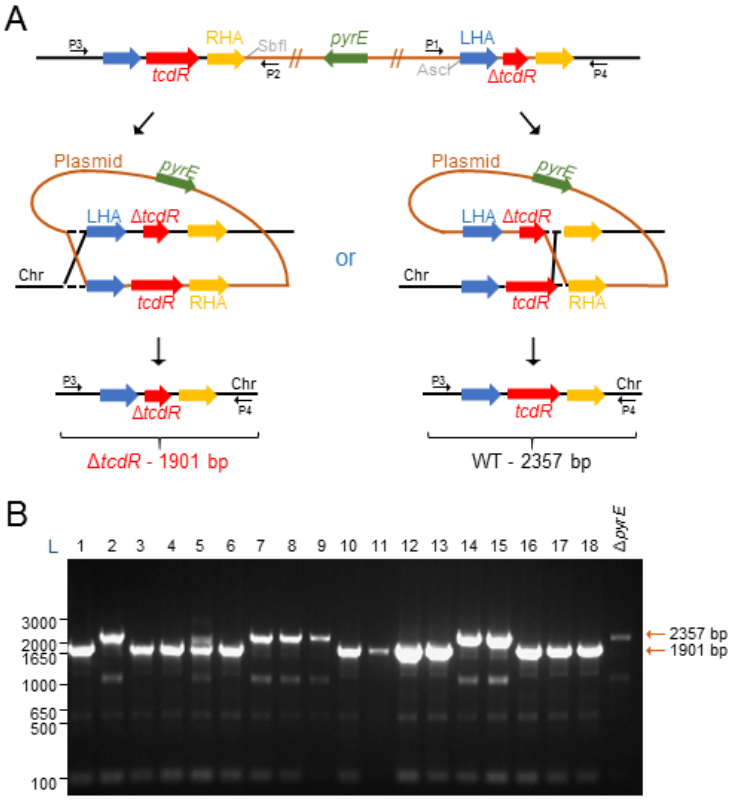

Figure 8 - ACE mutagenesis of *tcdR* gene in the 630Δ*erm*Δ*pyrE* strain. A: The goal of this mutagenesis is to replace the wild type gene by the truncated version. After integration, plasmid excision could leave the truncated gene in the chromosome or the wild type gene. The only way to distinguish between the two possibilities is to run a PCR using P3 and P4 primers. Chr, chromosome; B: Double cross-over mutant verification. P3: *tcdR*-vef-Fw; P4: *tcdR*-vef-Rev. 1 – 18: tested clones. L: 1 Kb Plus DNA ladder. The wild type gene has 2357 bp while the mutated one has 1901 bp. Therefore, from the 18 clones, 11 have the Δ*tcdR* mutation.

On the isolated *tcdR* mutant, the *pyrE*$^{-}$ gene was converted back to *pyrE*$^{+}$ using plasmid pMTL-YN1 (Ng *et al.*, 2013) as described in the material and methods section. The presence of the wild type *pyrE* gene was confirmed by PCR using primers *pyrE*-vef-Fw and *pyrE*-vef-Rev that anneal to the upstream and the downstream sequence of *pyrE*, respectively (Figure 9A). Using these primers, the strain 630Δ*erm*Δ*pyrE*Δ*tcdR* should give rise to a PCR fragment of 7056 bp, caused by the insertion of the Lambda phage 6.5 Kb in the *pyrE* locus (Heap *et al.*, 2012; Figure 9A). All the colonies tested were positives for *pyrE* reversion, since they generated a PCR fragment of 664 bp equal to the one

obtained using DNA from strain 630Δ*erm* (Figure 9B). Colony 1 was selected to the further studies (630Δ*erm*Δ*tcdR*; Appendix 2).

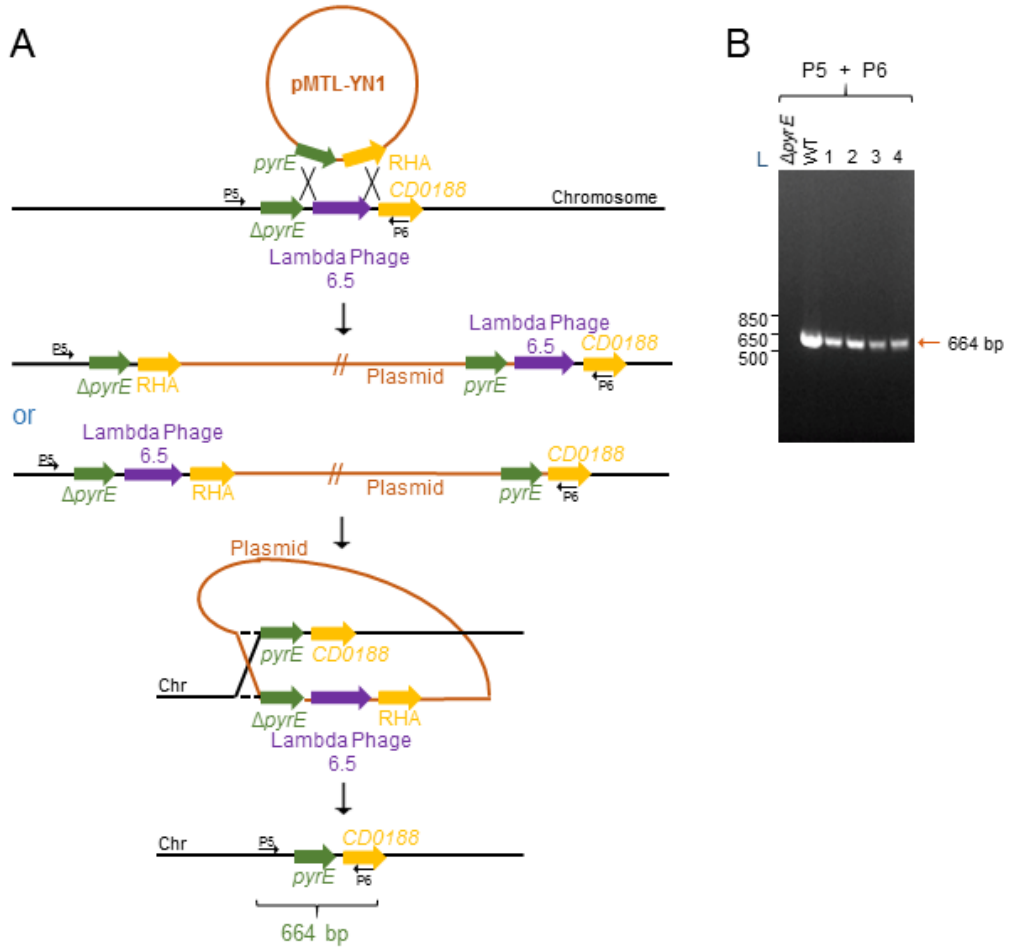

Figure 9 - *pyrE* reversion using the ACE system. A: In this case, reversion of the *pyrE*$^{-}$ allele to the WT is seeked in the 630Δ*erm*Δ*pyrE*Δ*tcdR* strain. The pMTL-YN1 has the wild type *pyrE* and a right homology arm (RHA). The goal is to integrate the plasmid and then excise it leaving in the chromosome the wild type *pyrE*. Only one of the four options fit the requirements. To confirm that the *pyrE* was reverted, P5 and P6 are used in a PCR reaction. Chr: Chromosome; B: *pyrE* reversion analysis. P5: *pyrE*-vef-Fw; P6: *pyrE*-vef-Rev. 1-4: tested clones. L: 1 Kb Plus DNA ladder. All the tested clones were *pyrE* revertants since the fragment size is the same as the one from the WT (630Δ*erm*) strain (664 bp). There is no amplification of the 630Δ*erm*Δ*pyrE* strain because the *pyrE* gene is interrupted by the Lambda Phage 6.5, which is too large to be amplified in this reaction.

Since our original strain 630Δ*erm*Δ*pyrE*Δ*tcdR* also has a specific in-frame deletion of the *pyrE* locus, ACE can be used to introduce a wild type copy of the *tcdR* gene into the chromosome at the *pyrE* locus concomitant with the correction of this allele back to the WT (PyrE^{+} phenotype). To complement the *tcdR* mutation the coding sequence of *tcdR* and its expected promoter region was amplified by PCR using primers *tcdR*-comp-BamHI-Fw and *tcdR*-comp-HindIII-Rev (Appendix 4). The resulting 1479 bp fragment

(bases 785783 to 787243 on the forward strand of *C. difficile* 630Δ*erm* genome) was digested with BamHI and HindIII and cloned in pMTL-YN1C (Ng *et al.*, 2013) digested with the same enzymes, to create pSR5 (Appendix 5). pSR5 was transferred to the 630Δ*erm*Δ*pyrE*Δ*tcdR* strain by conjugation. Transconjugants were selected on minimal medium plates. Three independent PyrE^{+} clones able to grow on minimal medium, in the absence of uracil, were screened for the presence of the wild type allele by PCR, using primers *pyrE*-vef-Fw and *pyrE*-vef-Rev (Figure 10A). Only clones 2 and 3 gave the expected 2404 bp DNA product (Figure 10B). Clone 3 was the selected for further studies (630Δ*erm*Δ*tcdR*, *pyrE*::*tcdR*; Appendix 2). The strain with the *in trans* copy of *tcdR* at the *pyrE* locus will be referred to as Δ*tcdR*^{C} for simplicity.

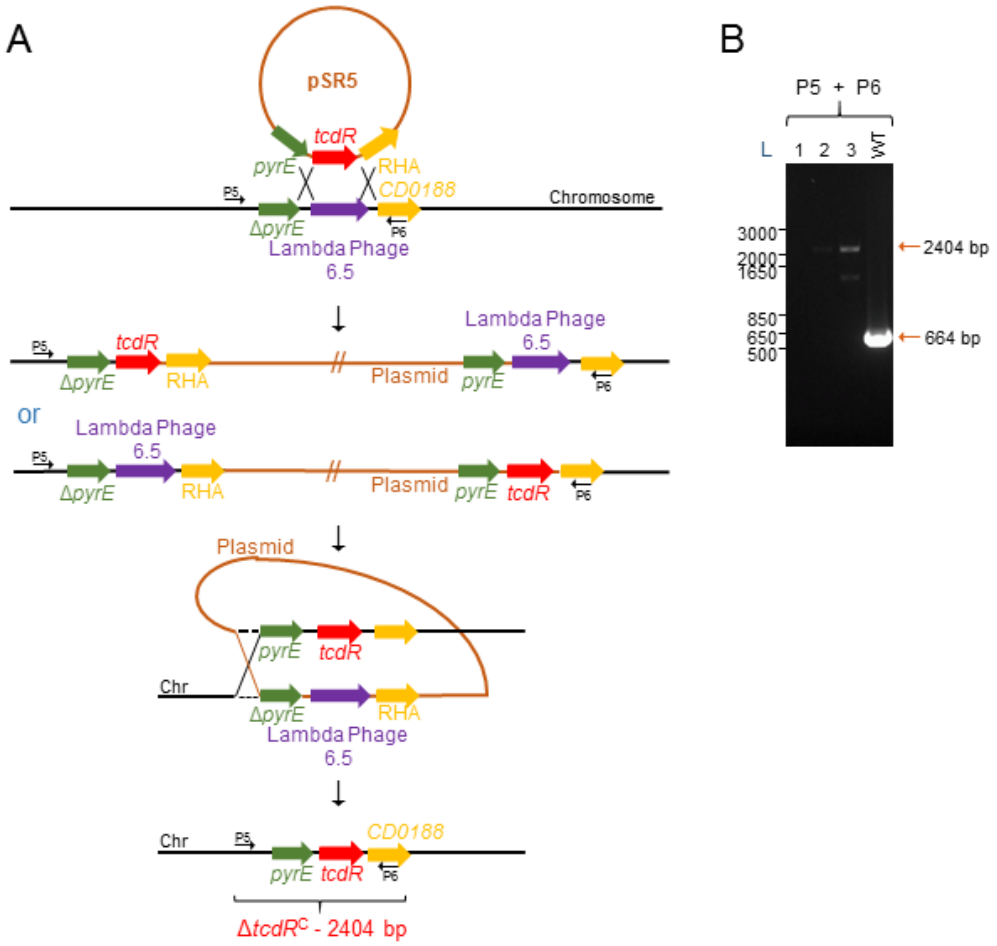

Figure 10 - *tcdR* complementation using the ACE system. A: *in trans* complementation of the *tcdR* allele in the 630Δ*erm*Δ*pyrE*Δ*tcdR* strain. The pMTL-YN1C has the wild type *pyrE*, the wild type *tcdR* and a right homology arm (RHA). The goal is to integrate the plasmid at the *pyrE* locus and excise it, leaving in the chromosome the wild type *pyrE* and the functional *tcdR*. Only one of the four options fit in the requirements. Chr: Chromosome; B: *tcdR* complementation confirmation in the 630Δ*erm*Δ*pyrE*Δ*tcdR* strain. P5: *pyrE*-vef-Fw; P6: *pyrE*-vef-Rev. 1-3: tested clones. L: 1 Kb Plus DNA ladder. If the gene was inserted in the *pyrE* locus as desired, the PCR fragment resulting from the *pyrE* verification primers would have 2404 bp; if not, the PCR reaction would produce a 664 bp fragment, as for the WT strain (630Δ*erm*). In order to simplify, the complemented strain will be referred to as Δ*tcdR*^{C}.

3.2. The *tcdR* mutation does not affect growth or sporulation

To analyse the impact of the *tcdR* mutation on bacterial growth, the WT strain (630Δ*erm*), the *tcdR* mutant, and the complementation strain were grown in TY and the optical density of the cultures was measured at 600 nm hourly until hour 12 after inoculation. As a control, the double Δ*tcdA*Δ*tcdB* mutant was grown in parallel (630Δ*erm*Δ*tcdA*Δ*tcdB*; Kuehne *et al.*, 2010). All three strains, WT (630Δ*erm*), Δ*tcdR* and the Δ*tcdR*^{C}, have similar growth rates (0.5513 h^{-1}, 0.5732 h^{-1} and 0.5527 h^{-1}, respectively) and, about 8 hours after inoculation, they enter in stationary phase that is prolonged at least until hour 24 (Figure 11A). Therefore, deletion of *tcdR* has no impact on the growth rate of *C. difficile* at least under our culturing conditions. The double mutant Δ*tcdA*Δ*tcdB* presented a lower growth rate when compared with the WT strain (0.4649 h^{-1} versus 0.5513 h^{-1}) and did not reach the same density as the other three strains. A similar observation was previously reported (Govind and Dupuy, 2012) and may be explained by cell lysis caused by the presence of TcdE (holin-like protein, see below) in the absence of the toxins. Since TcdR is the positive regulator of expression of the PaLoc, neither the toxin-encoding genes nor *tcdE* are expressed in the *tcdR* mutant. Perhaps for this reason, lysis was not observed.

A

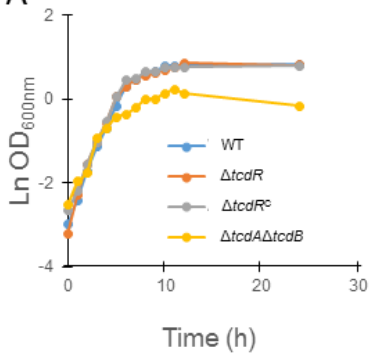

B

Strain (genotype)	Growth Rate (h^{-1})	Generation time (h)
WT	0.5513	1.2574
Δ*tcdR*	0.5732	1.2092
Δ*tcdR*^{C}	0.5527	1.2542
Δ*tcdA*Δ*tcdB*	0.4649	1.4909

Figure 11 - Growth curves of the WT (630Δ*erm*), Δ*tcdR*, Δ*tcdR*^{C} and Δ*tcdA*Δ*tcdB* strains. A: The OD of the cultures was measured at 600nm hourly until the 12th hour following inoculation and then, at hour 24. All strains presented similar growth rates and, with the exception of the Δ*tcdA*Δ*tcdB* mutant, they all reached similar maximum OD levels. The reason for the different behaviour observed for the double mutant remains to be elucidated (but see text); B: Growth rates and generation times for each strain.

Since previous work from the laboratory (Figure 6) showed that *tcdR* expression occurs mostly inside the forespore, it seemed possible that TcdR could have a role in sporulation. To understand if this was the case, the mutant and the respective complementation strain were analysed for their ability to form heat resistant spores. Strains were grown in SM, a medium in which we found sporulation to be more synchronized (Pereira *et al.*, 2013), and 24, 48 and 72 hours after inoculation the titer of heat resistant spores/ml of culture was determined (see the material and method section). In line with earlier results (Pereira *et al.*, 2013), the titer of spores for the WT strain increased from $6.8x10^5$ spores/ml of culture at hour 24, to $1.8\ x10^6$ spores/ml at hour 48 and $1.4x10^6$ spores/ml at hour 72 (Table 1). As expected from previous results (see above), the *tcdR* mutation did not affect cell viability (Table 1). Moreover, the titer of spores in the *tcdR* mutant was similar to the titer of WT spores, $2.3x10^6$, $5.4x10^6$ and $4.4x10^6$ spores/ml at hour 24, 48 and 72, respectively (Table 1).

Table 1 - Sporulation efficiency of the *tcdR* mutant and complementation strain, in comparison to the WT, 24, 48 and 72 hours following inoculation into SM. The analysis is based on the cfu/ml that are generated before and after treatment at 60ºC. The results are from a representative experiment; the standard deviation is also presented and results from three technical replicates.

	24h		**48h**		**72h**	
	Total viable cells	Heat resistant cells	Total viable cells	Heat resistant cells	Total viable cells	Heat resistant cells
WT	$1.8x10^8 \pm 9.4x10^7$	$6.8x10^5 \pm 2.4x10^5$	$2.5x10^7 \pm 9x10^6$	$1.8x10^6 \pm 5.3x10^5$	$3.4x10^7 \pm 6{,}2x10^6$	$1.4x10^6 \pm 5.7x10^5$
Δ*tcdR*	$1.1x10^8 \pm 4x10^7$	$2.3x10^6 \pm 1.2x10^6$	$3.2x10^7 \pm 7x10^6$	$5.4x10^6 \pm 9.2x10^5$	$2.9x10^7 \pm 6x10^6$	$4.4x10^6 \pm 9x10^5$
Δ*tcdR*^{C}	$1.1x10^8 \pm 8.1x10^6$	$8.4x10^5 \pm 2.8x10^5$	$4.6x10^7 \pm 9.1x10^6$	$1{,}2x10^6 \pm 1.9x10^5$	$2.4x10^7 \pm 5x10^6$	$1.2x10^6 \pm 3.2x10^5$

Together these results show that the absence of the main positive regulator of expression of the PaLoc, TcdR, does not affect growth or sporulation of *C. difficile*.

3.3. The role of TcdR in expression of the PaLoc genes

To study the role of *tcdR* as the regulator of the PaLoc expression at the single cell level, we used the SNAP^{Cd}-*tag* system. With that purpose, the *tcdR* mutant and the complementation strain were conjugated with plasmids containing the *tcdR* or *tcdA* promoter regions fused to the *SNAP*^{Cd}*-tag* (Appendix 2). These two promoters were chosen to investigate the role of TcdR on expression of the gene coding for toxin A (NB: previous work has shown that the signal obtained from P$_{tcdB}$-SNAP^{Cd} is very weak) as well as the auto-regulation of *tcdR* expression. Strains were grown in TY for 24 hours, labelled with the SNAP^{Cd}-*tag* substrate TMR-Star and imaged by fluorescence microscopy.

As previously observed (Figure 6), expression of P$_{tcdR}$-*SNAP*^{Cd} is detected in 5.8% of the vegetative cells of the wild type and in 32% of the sporulating cells, of which 31.7% show forespore-specific expression (Figure 12A and B). The *tcdR* mutant shows forespores-specific expression in 36.1% of the sporulating cells, and the complementation strains shows forespore-specific expression of P$_{tcdR}$-*SNAP*^{Cd} in 30.4% of the sporulating cells. A quantitative analysis of the fluorescence signal per cell shows similar levels of fluorescence in individual cells of the three strains (Figure 12C). In contrast, the population of cells showing fluorescence in vegetative cells of the *tcdR* mutant and the complementation strain is slightly decreased (Figure 12B) when compared to the WT (0.6 % for the mutant and 0.5 % for the complementation strain). However, the quantitative analysis of the individual cells showing a fluorescence signal shows similar levels of intensity (Figure 12C).

We conclude that deletion of *tcdR* does not significantly curtail expression from its own promoter. Our results point for a minor role of the postulated positive auto-feedback loop of *tcdR* (Mani *et al.*, 2002).

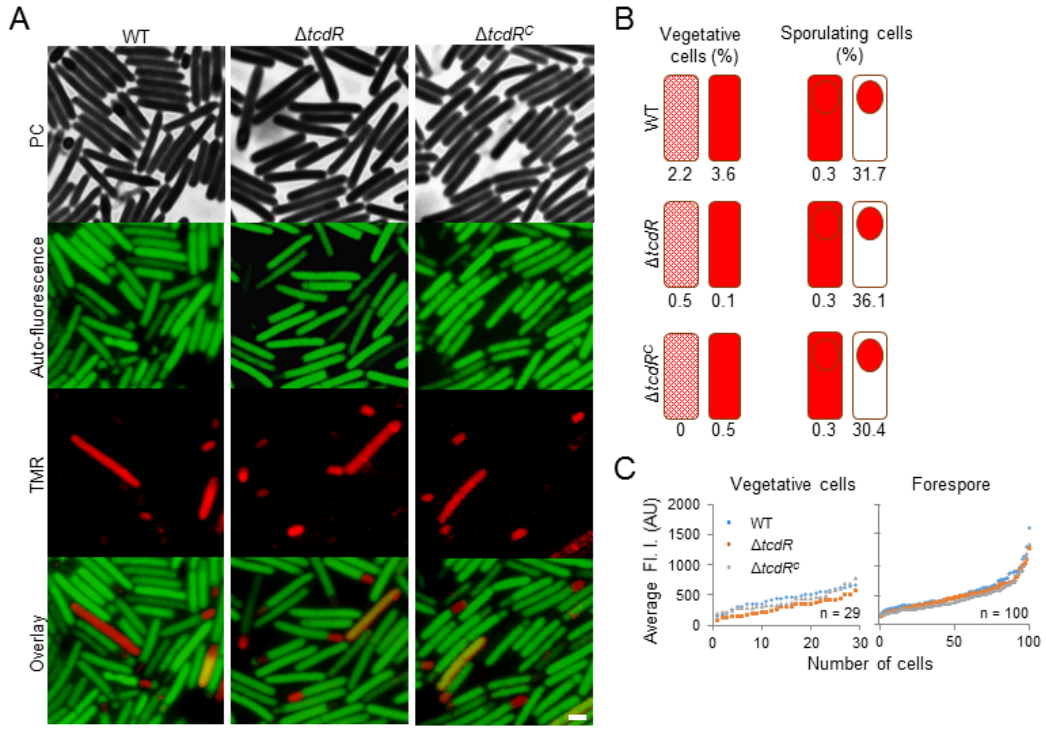

Figure 12 - TcdR is not essential for *tcdR* transcription. A: Fluorescence microscopy results for the WT (630Δ*erm*), the Δ*tcdR* and the Δ*tcdR*^{C} strains. These strains have a replicative plasmid with the *tcdR* promoter fused to the SNAP^{Cd}-*tag*. The cells were labelled with the red TMR substrate (benzylguanine derivative coupled to the tetramethylrodamine fluorophore). *C. difficile* cells show green auto-fluorescence. The overlay corresponds to the auto-fluorescence and TMR images. Phase contrast (PC) images are also shown. Scale bar: 1 µm; B: Cells counting from the microscopy results. These values are separated in vegetative cells (with low and high signal) and sporulating cells (with signal in whole cell or only in the forespore); C: Quantification of the signal (Average fluorescence intensity in arbitrary units, or AU) in vegetative cells and inside the forespore at initial sporulation stages (from septum formation to phase dark spores development). The WT is represented by the blue dots, the Δ*tcdR* mutant by the orange dots and the complemented strain by the grey dots.

In agreement with previous results of the laboratory (Figure 6), expression of P$_{tcdA}$-*SNAP*^{Cd} is detected in 76% of the vegetative cells and in 78.8% of the sporulating cells for the WT (Figure 13A and B). In sporulating cells, two patterns of P$_{tcdA}$-*SNAP*^{Cd} expression were seen: in one, the fusion was expressed only in the forespore in 0.17% of the sporulating cells; a second pattern corresponded to sporangia in which expression of the fusion was detected in both the mother cell and the forespore (78.6% of the sporulating cells). P$_{tcdA}$-*SNAP*^{Cd} expression is not detected in any of the cell populations in the *tcdR* mutant (Figure 13). In contrast, in the complementation strain, the number of cells showing fluorescence and the fluorescence intensity per cell was restored to nearly WT levels (Figure 13C): 75.6% of the vegetative cells, 0.47% in the forespore, and 92.2% in whole sporangia. Thus, the *tcdR* copy present at the *pyrE* locus restored P$_{tcdA}$-*SNAP*^{Cd} expression to the *tcdR* mutant. The phenotype of the mutant is thus due to loss of function of the *tcdR* gene.

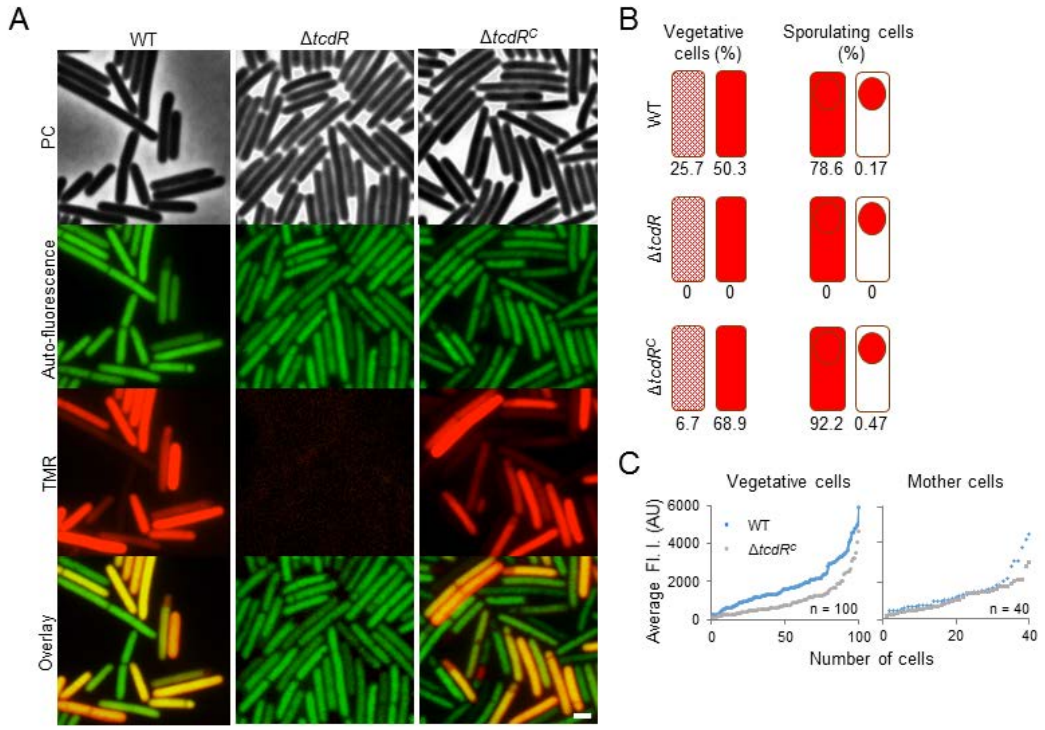

Figure 13 - TcdR protein is necessary for *tcdA* transcription. A: Fluorescence microscopy analysis of the WT (630Δ*erm*), the Δ*tcdR* and the Δ*tcdR*^{C} strains, bearing a replicative plasmid with the *tcdA* promoter fused to the SNAP^{Cd}-*tag*. The cells were labelled with the red SNAP^{Cd} substrate TMR-Star. Note that no signal is detected in the *tcdR* mutant. *C. difficile* cells show green auto-fluorescence. The overlay corresponds to the autofluorescence and TMR images. Phase contrast (PC) images are also shown. Scale bar: 1 µm; B: Scoring of the cells according to the indicated classes: vegetative cells (with low and high signal) and sporulating cells (with signal in whole cell or only in the forespore); C: Quantification of the fluorescence signal (Average fluorescence intensity, in arbitrary units, or AU) in vegetative cells and in the mother cells. The WT is represented by the blue dots and the complemented strain by the grey dots.

Together, the results confirm the requirement of TcdR for toxin production (or at least expression of the *tcdA* gene), but a minor role in the control of its own expression.

3.4. TcdA accumulates at the surface of spores

We found *tcdR* and *tcdA* to be expressed in the forespore, and we therefore anticipated accumulation of toxin A (TcdA) in the developing spore. Since the spore is hard to break, spore-specific expression of the toxin may have been missed until now. In order to further investigate association of TcdA with spores, we purified spores from the WT, the Δ*tcdR* mutant, the Δ*tcdR*^{C} strain, and from the Δ*tcdA*Δ*tcdB* mutant. Then, the coat proteins were extracted (coat fraction), and the decoated spores were submitted to lysozyme treatment. This treatment is thought to digest the exposed cortex releasing cortex-associated proteins (cortex fraction). Proteins from these fractions were resolved by SDS-PAGE and analysed by immunoblot using an anti-TcdA antibody (Figure 14).

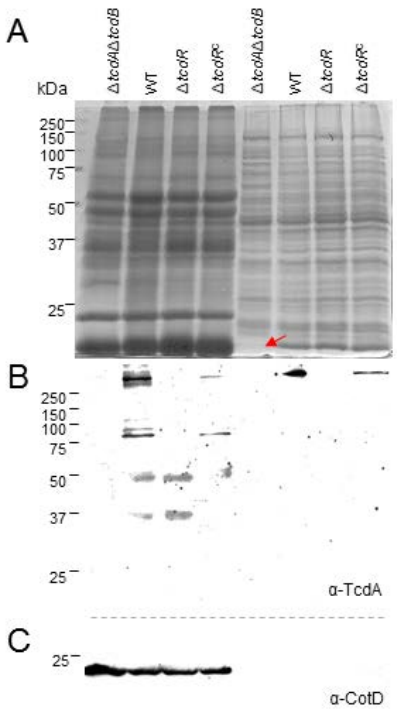

Figure 14 - TcdA accumulates at the spore surface. A: SDS-PAGE gel stained with coomassie brilliant blue. Four strains are compared: Δ*tcdA*Δ*tcdB*, WT (630Δ*erm*), Δ*tcdR* and Δ*tcdR*^{C}. The first four layers are coat protein extracts, whereas the last four lanes correspond to a cortex fraction (see text for details); B: Western blot analysis of the gel in A. The antibody was a mouse monoclonal anti-TcdA (from Santa Cruz Biotechnology); C: Reprobing of the membrane in B using a mouse polyclonal that recognizes the spore coat protein CotD (Permpoonpattana *et al*., 2011).

The profile and amount of proteins visualized by the gel stained with the coomassie brilliant blue solution is very similar among all strains except for the double mutant (Figure 14A). This strain did not show a protein migrating below the 25 kDa marker (Figure 14A, red arrow). Mass spectrometry analysis indicated that this species corresponds to a Rubrerythrin family protein (Rbr_1) with 20 kDa. The dependency on Δ*tcdA*Δ*tcdB* for assembly of the Rbr_1 protein was not investigated further.

In spores from the WT strain, the TcdA toxin (308 kDa) was detected in both the spore coat and cortex fractions. As expected, no TcdA was detected in spores from the *tcdR* mutant or the Δ*tcdA*Δ*tcdB* mutant. In the Δ*tcdR*^{C} strain, TcdA is also detected in both the coat and cortex fractions of the mature spore, although at slightly lower levels as compared to the WT (Figure 14B). As an indication of the decoating efficiency, the coat protein CotD (20 kDa; Permpoonpattana *et al.*, 2011) was present only in the coat fraction (Figure 14C). Presently, a protein to be used as a specific marker for the cortex fraction has not been identified. In any event, these results show that, at least, TcdA is associated with the surface of mature spores.

3.5. Construction and *in trans* complementation of an in-frame deletion mutant of *tcdE*

A previous study developed a *tcdE* mutant using the Clostron system (Govind and Dupuy, 2012). However, because this technique generates insertional mutations, the expression of downstream genes, such as *tcdA*, may be affected. Therefore, to decrease the possibility of polar effects, we constructed a *tcdE* mutant using the ACE mutagenesis system (Ng *et al.*, 2013). This mutant would allow us to investigate a possible function of TcdE on sporulation, since *tcdE* expression was detected inside the forespore in previous work of this laboratory (as detailed in the Introduction).

The ACE methodology (Ng *et al.*, 2013) was used to inactivate the *tcdE* gene. An allele exchange cassette was assembled composed of a left-hand homology arm (LHA) and a right-hand homology arm (RHA) relative to *tcdE*. The LHA (621 bp, which includes the last 386 bp of *tcdB*) was amplified by PCR using primers *tcdE*-AscI-Fw and *tcdE*-SOE-Rev (bases 794105 to 794695 on the forward strand of *C. difficile* 630Δ*erm* genome; Appendix 4). The RHA (590 bp) was amplified by PCR using primers *tcdE*-SOE-Fw and *tcdE*-SbfI-Rev (bases 795038 to 795615 on the forward strand of *C. difficile* 630Δ*erm* genome; Appendix 4). The two fragments were joined by splicing by overlap extension (SOE) PCR and cloned between the AscI and SbfI sites of pMTL-YN3 (Ng *et al.*, 2013) to produce pSR4 (Appendix 5). The fusion of the LHA with the RHA creates an in-frame deletion removing codons 28 to 141 of *tcdE* gene.

pSR4 was introduced in *C. difficile* 630Δ*erm*Δ*pyrE* (Appendix 2) by conjugation. The transconjugants obtained were restreaked two times in BHIS with thiamphenicol and cefoxitin to select for the single crossover. Large colonies were tested for pure single crossovers clones by PCR using two pairs of primers (Figure 15): pair 1 *tcdE*-vef-Fw (P3) and YN3-vef-Fw (P2), and pair 2 *tcdE*-vef-Rev (P4) and YN3-vef-Rev (P1). Depending which homology arm undergoes recombination, the PCR's from the single crossover will result with pair 1 in 1680 bp and pair 2 in 2022 bp fragments, or with pair 1 in 2049 bp and pair 2 in 1707 bp fragments (Figure 15A). Five colonies were shown by PCR to result

from single crossovers (colonies 2, 3, 4, 5 and 6; Figure 15B); colony 2 was selected to proceed with the mutagenesis.

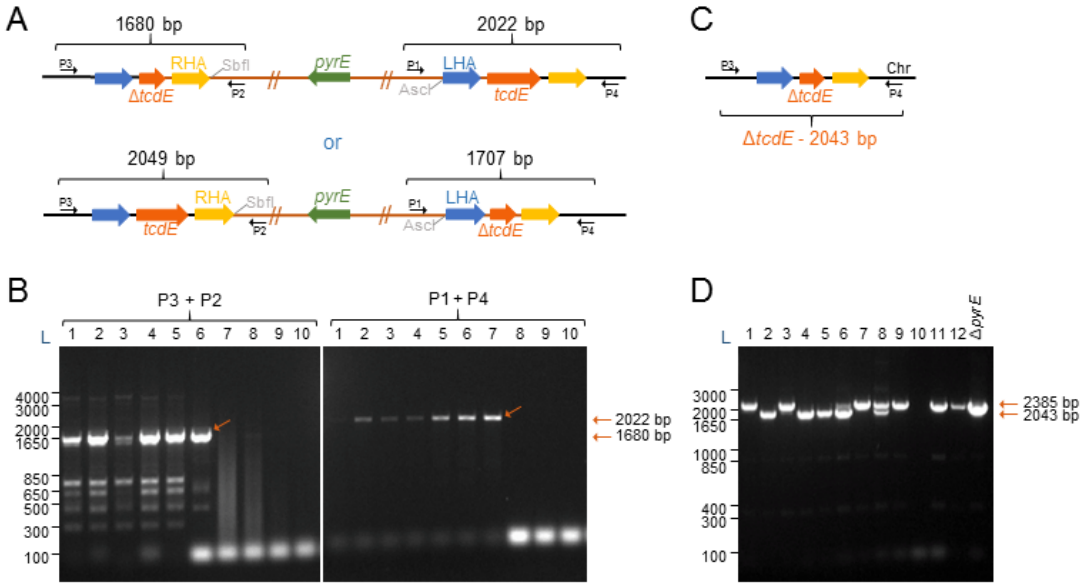

Figure 15 - ACE mutagenesis of the *tcdE* gene in strain 630Δ*erm*Δ*pyrE*. A: pSR4 can integrate in two different ways (see Figure 7) which can be distinguish using P3 and P2 in a PCR reaction and P1 and P4 in another. Chr, chromosome; B: Single cross-over analysis for *tcdE* mutagenesis. P3: *tcdE*-vef-Fw; P2: YN3-vef-Fw; P1: YN3-vef-Rev; P4: *tcdE*-vef-Rev. 1 to 10: tested clones. L: 1 Kb Plus DNA ladder. Clones number 2, 3, 4, 5 and 6 are positives since they presented the expected 1680 bp and 2022 bp fragments; C: The goal of this mutagenesis is to replace the wild type gene by the truncated version. After integration, plasmid excision could leave the truncated gene in the chromosome or the wild type gene (see Figure 8). The way to distinguish between the two possibilities is to run a PCR using P3 and P4 primers; D: Double cross-over mutant verification. P3: *tcdE*-vef-Fw; P4: *tcdE*-vef-Rev. 1-12: tested clones. L: 1 Kb Plus DNA ladder. Depending on the presence of the wild type gene or the truncated version, two fragment sizes are expected. The wild type gene has 2385 bp while the mutated one has 2043 bp. Therefore, from the 12 clones, 3 have the Δ*tcdE* mutation.

Single colonies were then re-streaked onto minimal medium supplemented with FOA and uracil to select for cells in which the integrated plasmid had excised. Depending which homology arm undergoes recombination, plasmid excision can result in either the desired double crossover mutant, or a wild type cell. The isolated FOA resistant colonies were then screened by PCR using primers *tcdE*-vef-Fw and *tcdE*-vef-Rev that anneal to the upstream and the downstream sequence of *tcdE*, respectively (Figure 15C). Of the 12 colonies screened, 3 yielded the expected 2043 bp DNA fragment, indicative of an in-frame deletion (2, 4 and 5; Figure 15D). The other colonies yielded a 2385 bp DNA fragment, consistent with the presence of a wild-type copy of the gene (Figure 15D). Colony 2 was chosen for further studies (630Δ*erm*Δ*pyrE*Δ*tcdE*; Appendix 2). Colonies 6 and 8 seemed to have both fragments, possibly because two colonies, instead of one, were used in the genomic DNA extraction, resulting in a mixed culture.

On the isolate *tcdE* mutant, the *pyrE*$^{-}$ gene was converted back to *pyrE*$^{+}$ using plasmid pMTL-YN1 (Ng *et al.*, 2013) as described in the material and methods section. The presence of the wild-type *pyrE* gene was confirmed by PCR using primers *pyrE*-vef-Fw and *pyrE*-vef-Rev that anneal to the upstream and the downstream sequence of *pyrE*, respectively (Figure 16A). Using these primers, strain 630Δ*erm*Δ*pyrE*Δ*tcdE* should give rise to a PCR fragment of 7056 bp, caused by the insertion of the Lambda phage 6.5 Kb in the *pyrE* locus (Heap *et al.*, 2012; Figure 9A). All the colonies tested were positives for the *pyrE* reversion, since they generated a PCR fragment of 664 bp equal to the one obtaining using the 630Δ*erm* strain (Figure 16B). Colony 1 was selected for further studies (630Δ*erm*Δ*tcdE*; Appendix 2).

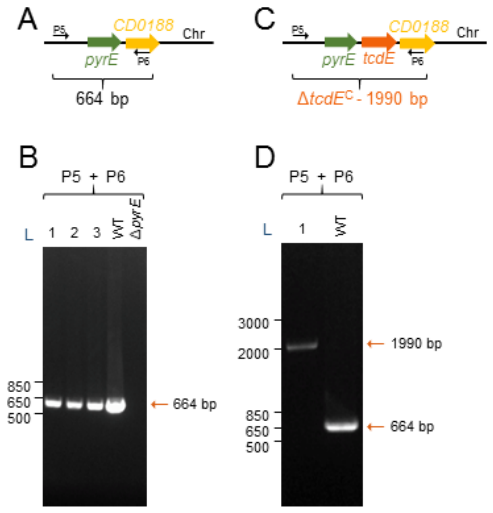

Figure 16 - *pyrE* reversion using the ACE system (A) and *in trans* complementation of *tcdE* in strain 630Δ*erm*Δ*pyrE*Δ*tcdE* (C). A: The goal is to restore the WT *pyrE* allele in strain 630Δ*erm*Δ*pyrE*Δ*tcdE*. To confirm that the WT *pyrE* allele was restored, P5 and P6 were used in a PCR reaction (see Figure 9). Chr, chromosome; B: *pyrE* reversion analysis. P5: *pyrE*-vef-Fw; P6: *pyrE*-vef-Rev. 1-3: tested clones. L: 1 Kb Plus DNA ladder. All the tested clones were *pyrE* revertants since the fragment size is the same as the one from the WT strain (664 bp); C: Schematic image of the *in trans tcdE* complementation at the *pyrE* locus. This was confirmed using P5 and P6 primers; D) *in trans* complementation of *tcdE* analysis. P5: *pyrE*-vef-Fw: P6: *pyrE*-vef-Rev. 1 – tested clone. L: 1 Kb Plus DNA ladder. If the gene was inserted at the *pyrE* locus as desired, the PCR fragment resulting from the *pyrE* primers would have 1990 bp; the WT fragment have 664 bp.

As explained before, we can use ACE to introduce a wild type copy of the *tcdE* gene into the chromosome at the inactivated *pyrE* locus concomitant with the correction of this allele back to a wild type *pyrE* gene (resulting in a PyrE^{+} phenotype). However, expression of *tcdE* from its own promoter using a multicopy plasmid was observed to be lethal to *C. difficile* (Govind and Dupuy, 2012) therefore, the anhydrotetracycline (ATc) inducible gene expression system was used to control the expression of *tcdE*. To complement the *tcdE* mutation, the coding sequence of *tcdE* together with the three

published Ribossome Binding Site's (Govind and Dupuy, 2012) were amplified by PCR using primers *tcdE*-comp-SacI-Fw and *tcdE*-comp-BamHI-Rev (Appendix 4). The resulting 543 bp fragment (794591 to 795115 on the forward strand of *C. difficile* 630Δ*erm* genome) was digested with SacI and BamHI and cloned in pFT46 (Pereira *et al.*, 2013; Appendix 5) cleaved with the same enzymes. Since this plasmid already carries the ATc-inducible promoter, the *tcdE* fragment was inserted downstream of it. The NheI and BamHI sites were used to clone all the fragment (*tcdE* under the control of the inducible promoter) in the *pyrE* locus of pMTL-YN1C (Ng *et al.*, 2013), resulting in pSR6 (Appendix 5).

pSR6 was transferred to 630Δ*erm*Δ*pyrE*Δ*tcdE* by conjugation. Transconjugants were selected on minimal medium plates. $PyrE^+$ clones able to grow on minimal media in the absence of uracil were screened for the presence of the wild type allele by PCR using primers *pyrE*-vef-Fw and *pyrE*-vef-Rev (Figure 16C). Clone 1 gave the expected 1990 bp DNA product (Figure 16D). The strain bearing the *tcdE*-inducible allele at the *pyrE* locus will be referred to as $\Delta tcdE^C$ (Appendix 2).

3.6. The *tcdE* mutation does not affect growth or sporulation

To analyse the impact of the *tcdE* mutation on the bacterial growth, the WT strain (630Δ*erm*), the *tcdE* mutant, and the complementation strain were grown in TY and the OD_{600} measured at hourly intervals until hour 12 following inoculation (Figure 17A). Because the complementation of *tcdE* demands induction by anhydrotetracycline (ATc), all strains were tested with and without ATc. Previous studies suggested that 20 ng/ml of ATc were suitable for complementation of *tcdE* (Govind and Dupuy, 1012). In this work, ATc concentrations of 20 ng/ml and 20 µg/ml were used herein. The higher concentration used in this work (20 µg/ml) was an attempt to force high levels of expression of *tcdE* and possibly a more clear lysis phenotype.

In the presence of 20 ng/ml of ATc, all the three strains, WT (630Δ*erm*), Δ*tcdE* and the $\Delta tcdE^C$, had similar growth rates (0.5493 h^{-1}, 0.5564 h^{-1} and 0.549 h^{-1}, respectively; Figure 17B) as well as without induction (0.5513 h^{-1}, 0.5413 h^{-1} and 0.5416 h^{-1}, respectively; Figure 17B). After about 8 hours, the cells enter into stationary phase at very similar ODs (Figure 17A). Therefore, under these conditions, the *tcdE* mutation or the

expression of *tcdE* from the ATc-inducible promoter, have no impact on growth of *C. difficile*.

A

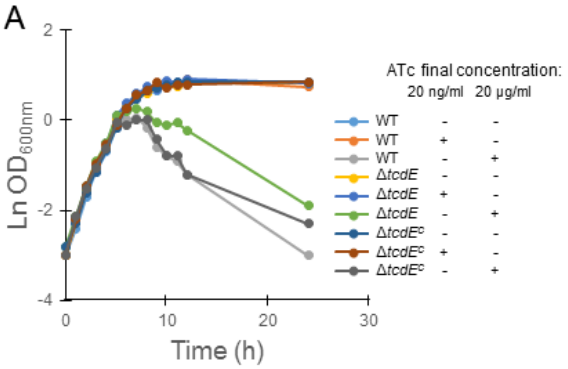

B

Strain (genotype)	Growth Rate (h^{-1})	Generation time (h)
WT	0.5513	1.2574
WT (20 ng/ml ATc)	0.5493	1.2619
WT (20 µg/ml ATc)	0.5728	1.2101
Δ*tcdE*	0.5413	1.2805
Δ*tcdE* (20 ng/ml ATc)	0.5564	1.2456
Δ*tcdE* (20 µg/ml ATc)	0.5431	1.2762
Δ*tcdE*^{C}	0.5416	1.2798
Δ*tcdE*^{C} (20 ng/ml ATc)	0.549	1.2626
Δ*tcdE*^{C} (20 µg/ml ATc)	0.4977	1.3928

Figure 17 – Growth curves of the WT, Δ*tcdE* and Δ*tcdE*^{C} strains. A: The OD was measured at 600 nm hourly until 12 hours after inoculation and then, at hour 24. Strains were induced with the indicated concentrations of ATc at the 4th hour of growth; B: Growth rates and generation times for each of the indicated strains.

In the presence of 20 µg/ml of ATc, growth was impaired for all three strains. Therefore, the lysis observed for the complemented strain cannot be directly attributed to increased expression of *tcdE* (Figure 17).

Since previous work from the laboratory (Figure 6) showed that the *tcdE* expression occurs mostly inside the forespore, we considered the possibility that this gene could have a role in sporulation. To test this possibility, the ability of the mutant to form heat resistant spores was assessed. Strains were grown in SM and after 24, 48 and 72 hours after inoculation, the titer of heat resistant spores/ml of culture was determined as described in the material and method section. In line with earlier results (Pereira *et al.*, 2013), the titer of spores for the wild type strain increased from $4.3x10^5$ spores/ml of culture at hour 24, to $1.2x10^6$ spores/ml at hour 48 and $1.7x10^6$ spores/ml at hour 72 (Table 2). As expected from the previous results (Figure 17A) the *tcdE* mutation did not affect cell viability (Table 2). Moreover, the titer of spores in the *tcdE* mutant was similar to the titer of WT

spores, $1.5x10^5$, $5.6x10^5$ and $9x10^5$ spores/ml at hour 24, 48 and 72, respectively (Table 2).

Table 2 - Sporulation efficiency of *tcdE* mutant strain, in comparison to the WT, 24, 48 and 72 hours following inoculation into SM. This analysis is based on the cfu/ml that are obtained on plates before and after heat treatment. The results are from a representative experiment; the standard deviation results from three technical replicates.

	24h		**48h**		**72h**	
	Total viable cells	Heat resistant cells	Total viable cells	Heat resistant cells	Total viable cells	Heat resistant cells
WT	$1.3x10^8 \pm 9.2x10^7$	$4.3x10^5 \pm 2.1x10^5$	$5.6x10^7 \pm 1x10^7$	$1.2x10^6 \pm 4.9x10^5$	$2.6x10^7 \pm 6{,}7x10^6$	$1.7x10^6 \pm 5.2x10^5$
Δ*tcdE*	$1.5x10^8 \pm 3.9x10^7$	$1.5x10^5 \pm 5.6x10^4$	$6.7x10^7 \pm 2.2x10^7$	$5.6x10^5 \pm 1.7x10^5$	$2.3x10^7 \pm 3.5x10^6$	$9x10^5 \pm 3.5x10^5$

Together, these results show that the absence of the holin-like protein, TcdE, does not affect growth or sporulation of *C. difficile*, in agreement with the results of a previous study (Olling *et al.*, 2012).

3.7. Absence of TcdE does not affect the release of TcdA from vegetative cells

The function of TcdE is controversial. Olling *et al.* (2012) showed that growth, sporulation and release of TcdA and TcdB from *C. difficile* strain 630 were not affected by inactivation of the *tcdE* gene. However, Govind and Dupuy (2012) argued that TcdE, an apparent holin, is required for efficient toxin secretion by *C. difficile*, but that it does so without causing significant cell lysis or membrane damage usually associated with phage holins. Toxin A was detected in the supernatant of vegetative cells in a WT strain whereas in the *tcdE::ermB* mutant, constructed using the Clostron system (Govind and Dupuy, 2012), the toxin was retained inside the cells (Govind and Dupuy, 2012). We investigated toxin secretion using our in-frame deletion Δ*tcdE* mutant.

After 4 hours of growth, *tcdE* expression in the complementation strain was induced for 2 hours with ATc (20 ng/ml). In parallel, ATc was added to the WT strain and the *tcdE* mutant. At the end of the induction period the cells were collected by centrifugation, and the presence of TcdA was investigated in the cell sediment and in the supernatant by dot blot using an anti-TcdA antibody. In one set of experiments, we used exactly the same conditions as described by Govind and Dupuy: at hour 6 of growth, the cells were collected, and the presence of TcdA in the two fractions was investigated. We found a weak signal for TcdA in the supernatant of all strains, which was only slightly above

background levels (estimated in the *tcdA*/*tcdB* double mutant). Moreover, we found no differences in the signal observed in the supernatant or the cell sediment between the stains under analysis (Figure 18A). These results suggest that TcdE has no major role in TcdA secretion, at least at this stage of growth, and are not in line with the results from the Govind and Dupuy study (Govind and Dupuy, 2012). In a second set of experiments, we examined the presence of TcdA in the supertant and the cell sediment prepared from cultures of the WT, the Δ*tcdE* mutant, the Δ*tcdE*^{C} strain and the double *tcdA*/*tcdB* mutant during entry into stationary phase, when transcription of *tcdA* and also of *tcdB* is known to increase (Hundsberger *et al.*, 1997). Samples were collected from cultures of the various strains 12, 16 and 20 hours after inoculation, with ATc (20 ng/ml) added at hour 10. The samples were fraccionated and 60 µg of total supernantant protein, and 10 µg of total cell sediment protein were analysed by dot blot. The results of this experiment is shown on Figure 18B; we found no difference in the level of TcdA in the supernatants and in the cell sediments prepared from the different strains at any of the time points tested. These results are in agreement with those of Olling and co-authors (Olling *et al.*, 2012) and suggest no major role for TcdE in secretion of TcdA.

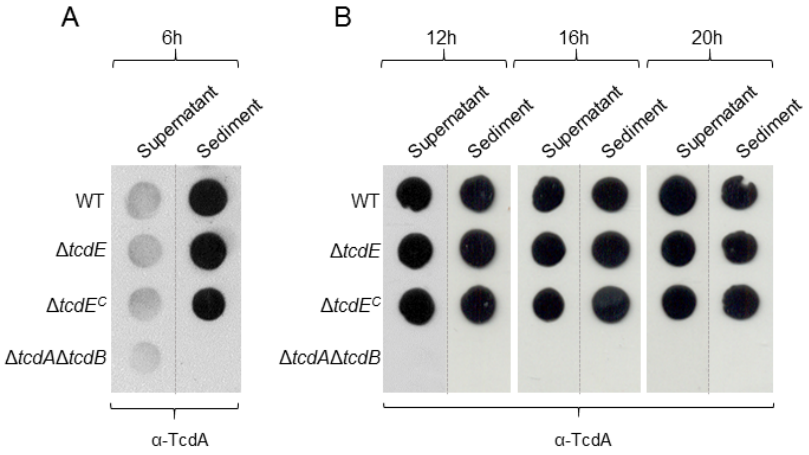

Figure 18 - TcdE has no major role in TcdA secretion from vegetative cells. A: detection of TcdA by dot blot in the supernant and cell sediment prepared from cultures of the WT, Δ*tcdE*, Δ*tcdE*^{C} and Δ*tcdA*Δ*tcdB* strains 6 hours following inoculation (see text for details). B: Dot blot assay using the supernatant and sediments prepared from cultures of the same strains as in panel A, but sampled 12, 16 and 20 hours following innoculation. Samples collected at hour 6 (panel A) were induced with 20 ng/ml of ATc at the hour 4 of growth; for the cultures in B, samples induction was carried out at hour 10 of growth. The supernatant was concentrated while cells from the sediment were lysed. In B, 60 µg of total protein were applied to the membrane for the supernatant sample, and 10 µg were analysed for the sediment sample (see text for details).

3.8. TcdE has no relevant role on the accumulation of TcdA in spores

We found *tcdE* to be expressed in the forespore, and since earlier results from this work (Figure 14) showed TcdA accumulation in the spore, we considered the possibility that TcdE could have a role on the localization of TcdA. The coat proteins were extracted from purified spores (coat fraction), and the decoated spores were subject to a lysozyme treatment that digested the exposed cortex and is thought to release cortex-associated proteins (cortex fraction). Proteins from these fractions were resolved by SDS-PAGE and analysed by immunoblot using an anti-TcdA antibody (Figure 19).

The profile and amount of proteins visualized by the gel stained with the coomassie brilliant blue solution was very similar between all strains (Figure 19A). This suggests that TcdE has no major role on the assembly of the spore coat.

In spores from the WT strain, the TcdA toxin (308 kDa) was detected in both the spore coat and cortex fractions. As expected, no TcdA was detected in spores from the Δ*tcdA*Δ*tcdB* mutant. The Δ*tcdE* mutant strain also presented TcdA in both the coat and cortex fractions, although the level of the toxin seemed slightly reduced (Figure 19B). Coat protein CotA (34 kDa; Permpoonpattana *et al.*, 2011) was only detected in the coat fraction (Figure 19C). Presently, no protein is known that can be used as a specific marker for the cortex fraction.

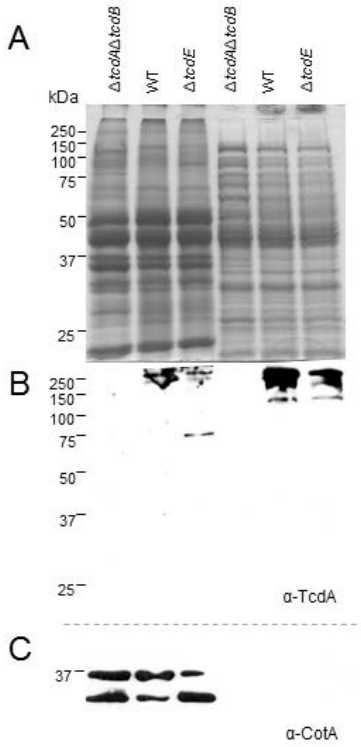

Figure 19 - TcdE has no relevant role on the accumulation of TcdA in spores. A: SDS-PAGE gel stained with coomassie brilliant blue. Three strains are compared: Δ*tcdA*Δ*tcdB*, WT (630Δ*erm*) and Δ*tcdE*.The first three layers are coat extracts, whereas the last three lanes correspond to a cortex fraction (see text for details); B: Western blot analysis of the gel in A, using a mouse monoclonal anti-TcdA antibody (from Santa Cruz Biotechnology); C: Reprobing of the membrane in B using a mouse polyclonal antibody against spore coat protein CotA (Permpoonpattana *et al*., 2011).

We conclude that TcdE plays no major role in the accumulation or localization of TcdA in mature spores.

4. Discussion and Conclusion

Using the recently described ACE mutagenesis technique (Ng *et al.*, 2013), we constructed two mutants, bearing in-frame deletion mutations of the *tcdR* or *tcdE* genes, and the corresponding *in trans* complementation strains. The Δ*tcdR* mutant was used to determine the impact of the mutation on expression of *tcdR* as well as the remaining PaLoc genes, during vegetative growth and during sporulation. The Δ*tcdE* mutant was constructed to assess the contribution of the *tcdE* gene for the release of the toxins from cells during growth and during sporulation, as well as its possible contribution for the localization of the toxins in mature spores.

The mutations did not affect the growth rate of the mutants, which suggests that neither TcdR nor TcdE are involved in cell viability (Figure 11 and 17). Moreover, no significant differences in the capacity to form spores were seen for the mutant strains in comparison to the WT (Table 1 and 2).

In a previous study, Govind and Dupuy have shown that a Δ*tcdA*Δ*tcdB* double mutant showed increased cell lysis during the transition to the stationary phase of growth as compared to the parental strain or PaLoc-negative strains (Govind and Dupuy, 2012). This effect was attributed to a possible role of the toxins in plugging the TcdE pore (Govind and Dupuy, 2012). We have also seen earlier lysis for the Δ*tcdA*Δ*tcdB* mutant in the background of strain 630Δ*erm* (Figure 11). In contrast, the Δ*tcdR* mutant, which does not produce toxin A (Figure 13) neither probably, any of the other PaLoc-encoded proteins including TcdE (Mani *et al.*, 2001), does not shows signs of lyse. These observations are consistent with the plugging model, which also suggests that a pore formed by TcdE is the key mechanism involved in the release of the toxins from the cells (Govind and Dupuy, 2012). However, complementation of the *tcdA* and *tcdB* mutations *in trans* was not reported in the study of Govind and Dupuy (Govind and Dupuy, 2012). A clean genetic demonstration of the plugging model would involve expression of *tcdE* and *tcdA/tcdB* under the control of different inducible promoters, so that lysis, in case the model is correct, would only occur when only *tcdE* is induced. Transplantation of the three genes to *B. subtilis*, more amenable to genetic manipulation, could facilitate these studies.

Previous work from our laboratory showed that the *tcdR* gene is transcribed in a fraction of vegetative cells, but also in sporulating cells (Figure 6). This important observation strongly suggests that the toxins are released from vegetative cells, at the onset of stationary phase, but accumulate in or associate with the developing spore. In any event, this observation shows a link between the processes of toxin production and spore differentiation.

In vitro studies suggest that expression of *tcdR* is under positive auto-regulation (Mani *et al.*, 2002): the regulatory region of the *tcdR* gene contains two promoters that are utilized by TcdR-containing RNA polymerase *in vitro*. An important question we addressed was whether auto-regulation of *tcdR* expression was important *in vivo*, in either vegetative or sporulating cells. If *tcdR* expression was under strong positive auto-regulation, we expected the Δ*tcdR* mutation to severely curtail transcription of a P_{tcdR}-*SNAP*^{Cd} fusion. Strong positive auto-regulation can lead to the bifurcation of the population into two sub-populations, one above and the other below the threshold for auto-activation (Alon, 2007). Strong positive auto-regulation of *tcdR* expression in vegetative cells was expected because the preliminary results in the group showed that some cells expressed *tcdR* while other did not (see the Introduction; see also Figure 6).

However, our results indicate that TcdR plays no relevant role in the expression of *tcdR* in either vegetative or sporulating cells at least under our culturing conditions (Figure 12). Presumably then, another factor is responsible for the observed bifurcation of the population with respect to *tcdR* expression. The answer may be in a third potential promoter located in the *tcdR* regulatory region, which is SigD-dependent. SigD is a sigma factor required for assembly of the flagellum and for motility and is thought to positively control toxin gene expression in vegetative cells by directly activating transcription of *tcdR* (El Meouche *et al.*, 2013; Figure 20). Other results from the laboratory indicate that deletion of *sigD* as well as point mutation in the -10 element of the SigD-dependent promoter, significantly reduced expression of *tcdR* or *tcdA* in vegetative cells. SigD is not directly involved in sporulation (El Meouche *et al.*, 2013) and accordingly, deletion of *sigD* did not eliminate forespore-specific expression of *tcdR.* However, we hypothesized that the SigD dependent promoter could also be utilized by regulatory proteins specific to the forespore. This appears to be the case, in fact, because point mutations in the -10 region of the SigD-dependent promoter eliminated forespore-specific expression of *tcdR*

in the forespore. The SigD-dependent promoter may be utilized by SigG with the help of SpoVT, because: *i*) in *E. coli*, it is only when the two proteins are co-produced that a reporter for *tcdR* expression is produced; *ii*) production of the reporter is not detected when SigG and SpoVT are co-produced but expression of *tcdR* is under the control of the mutant SigD-type promoter. SigG together with the ancillary transcription factor SpoVT appear to ensure robust expression of *tcdR* in the forespore; *tcdR* expression was detected mostly in the forespore (Figure 12). Production of SpoVT is under the control of SigG (Saujet *et al.*, 2013). Therefore, SigG and SpoVT define a coherent feed-forward loop (FFL) with AND gate logic that controls the expression of *tcdR* in the forespore. This circuit may have two consequences for production of TcdR in the forespore. First, production of TcdR may rely on signals that control the production and the activity of both SigG and SpoVT. For SigG, morphological signals may be involved, as the activity of SigG increases following engulfment completion (Pereira *et al.*, 2013). The signals, if any, that control the activity of SpoVT, are not known. However, we note that the protein has a GAF domain, and may thus bind small molecules, including amino acids (Dong *et al.*, 2004; Asen *et al.*, 2009). Secondly, since activation of *tcdR* transcription depends on the accumulation of SpoVT above a certain threshold level, the FFL acts to delay the expression of the PaLoc in the forespore. Toxin production has a high energy cost (Aktories *et al.*, 2000). We hypothesize that in this manner, the cost associated with the production of the two toxins is minimized.

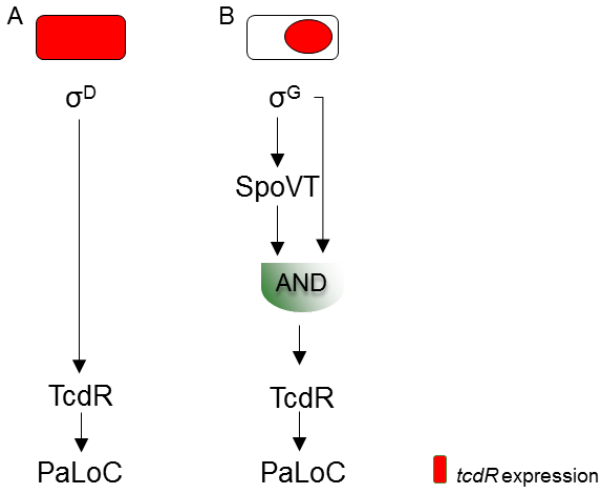

Figure 20 – Regulatory circuits governing *tcdR* expression. A: SigD is thought to positively control toxin gene expression in vegetative cells by directly activating transcription of *tcdR* (El Meouche *et al.*, 2013); B: In the forespore, SigG and SpoVT probably define a coherent feed-forward loop (FFL) with AND gate logic that controls the expression of *tcdR*. No contribution of auto-regulation for *tcdR* expression under our conditions was detected.

While TcdR appeared essential for the expression of *tcdA* (Figure 13), most of the *tcdR* signal was confined to the forespore, whereas most of the *tcdA* signal was detected in vegetative and in the mother cell of sporulating cells (Figures 12 and 13). One possible explanation for this discrepancy may be that low expression of *tcdR*, difficult to detect and quantify under our experimental conditions, is sufficient for activation of *tcdA* transcription. In *C. botulinum* expression of *botR*, coding for an alternative RNA polymerase sigma factor required for expression of the gene, *botA*, coding for the botulinum neurotoxin A, was about 100-fold less than that of the *botA* gene (Couesnon *et al.*, 2006). Thus, it appears possible that low levels of expression of the gene coding for the regulators of toxin expression are sufficient to generate high levels of expression of the toxin genes also in *C. difficile*.

However, and as discussed above, the different levels of *tcdR* expression in vegetative cells may also be part of the reason why some vegetative cells show high expression of *tcdA* while other show low levels of *tcdA* transcription.

Expression of *tcdA* is also detected in the mother cell of sporulating cells. Deletion of *sigD* eliminates this population (unpublished results of the laboratory), suggesting that some SigD remains active in the mother cell following asymmetric division. However, expression of *tcdA* in the forespore, was strictly dependent on *tcdR*, and on the forespore-specific production of SigG and SpoVT (Figure 20).

Complementation of the *tcdR* mutation in single copy at the *pyrE* locus almost totally restored the phenotype of the WT (Figures 12, 13 and 14). The small differences noticed may perhaps result from the absence of important sequences upstream or downstream of the *tcdR* fragment used for complementation. While further work is required to investigate this point, the overall conclusion of the complementation experiments is that the phenotype detected at the level of *tcdA* expression can be attributed mainly, if not exclusively, to the absence of TcdR.

We assume that the conclusions relative to the expression of *tcdA* at the single cell level can be extended to *tcdB.* However we note that the level of expression of *tcdB* was much lower than that of *tcdA*. This precluded a detailed analysis of *tcdB* expression in vegetative as well as in sporulating cells.

The forespore-specific expression of *tcdA* may result in the accumulation of TcdA in the forespore, and the rapid release of at least some TcdA during spore germination. This

may be an advantage during infection; low levels of toxin can trigger inflammation, which in turn promotes colonization. Release of the toxin during spore germination could rapidly provide sufficient toxins to promoter efficient colonization by the cell resulting from spore germination, which would not have to wait for toxin production and secretion (Figure 21; see also below). It will be interesting to determine whether TcdA is released, following spore germination, from outgrowing cells.

An important discovery was the association of TcdA with the spore. In strain 630Δ*erm*, TcdA was found mainly associated with the spore coat, although some toxin was also found in a cortex fraction (Figure 14). The association of TcdA with the spore surface layers implies that the infectious spore already carries the toxin. This was the first time that *C. difficile* toxins were shown to associate with mature spores, more specifically with the surface layers of the spore. In *C. perfringens* the spore forming and the toxin producing cells also overlap, but enterotoxin production may be under the control of mother cell-specific regulatory proteins (Ohtani *et al.*, 2013). Ungerminated *B. anthracis* spores also contained a detectable level of toxin components (Cote *et al.*, 2005). It will be of pivotal importance to understand the biological relevance of a spore packed with toxins during the infectious cycle of *C. difficile*. One possibility is that the localization of TcdA at the surface of spores is required for efficient binding of the spore to the colonic mucosa, possibly to the same receptor recognized by TcdA. It is also possible that the toxin, partially exposed at the spore surface, is important to trigger inflammation, and facilitate colonization (see also preceding section). In any event, the levels and exact location of the TcdA in spores vary among epidemic strains, helping to explain their epidemiological profile. Further studies are required to test these ideas.

The finding that TcdA is associated with the coat and cortex of mature spores raises the question of how it gets there. One possibility is that the TcdA is produced in the mother cell, at least in some of the sporulating cells, and it is recruited to the spore surface during the assembly of the spore cortex and coat sub-structures (Figure 21A). However, a different possibility is that the forespore-specific expression of *tcdA* also leads to the accumulation of TcdA at the spore surface. In this case, the implication would be that some of the toxin would have to be transported to the spore surface. In this scenario, we speculated that, perhaps, TcdE could be involved in the relocation of TcdA to the spore

surface (Figure 21B). However, accumulation of TcdA and its localization in mature spores was not affected significantly in Δ*tcdE* spores (Figure 19).

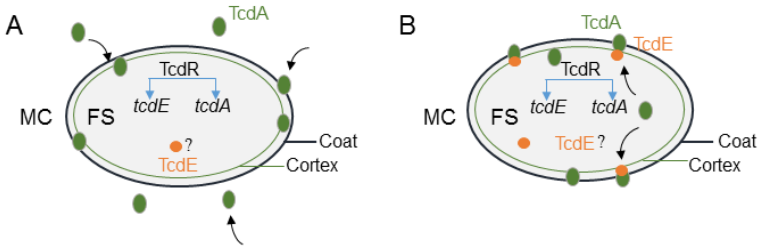

Figure 21 – Two posssible mechanisms for TcdA accumulation at the spore surface. A: TcdA is produced in the mother cell, at least in some of the sporangia cells, and it is recruited to the spore surface during the assembly of the spore cortex and coat sub-structures; and/or B: The forespore-specific expression of *tcdA* also leads to the accumulation of TcdA at the spore surface by an unknown mechanism. MC: Mother cell; FS: Forespore.

Previous work suggests a key role for TcdE in the release of TcdA and TcdB from *C. difficile* cells (Govind and Dupuy, 2012). We investigated whether we could reproduce this observation using our *tcdE* in-frame deletion mutant resulting from the ACE mutagenesis. However, we found no differences between the mutant strain Δ*tcdE* and the WT in what concerns the level of TcdA in the supernatant or cell-associated, at different stages of growth or sporulation. Thus, our results seem more consistent with other studies, in which TcdE was found not to have an impact on toxins release from the cells (Olling *et al.*, 2012). While the role of TcdE in expression of the virulence phenotype remains unclear, an experiment that could be informative is to test for a role of TcdE in TcdA release from outgrowing cells, resulting from spore germination.

The relationship between spore formation and toxin production by *Clostridium difficile* is essential to understand the infectious process and the epidemiological profile of various strains. Our study makes a first contribution towards this end.

5. References

Abecasis, A. B., M. Serrano, R. Alves, L. Quintais, J. B. Pereira-Leal, and A. O. Henriques. 2013. A genomic signature and the identification of new endosporulaion genes. Journal of Bacteriology. **195**(9): 2101–15.

Akerlund, T., B. Svenungsson, A. Lagergren, and L. G. Burman. 2006. Correlation of disease severity with fecal toxin levels in patients with *Clostridium difficile*-associated diarrhea and distribution of PCR ribotypes and toxin yields *in vitro* of corresponding isolates. Journal of Clinical Microbiology. **44**: 353–358.

Alon, U. 2007. Network motifs: theory and experimental approaches. Nature Reviews Genetics. **8**: 450-461.

Antunes, A., I. Martin-Verstraete, and B. Dupuy. 2011. CcpA-mediated repression of *Clostridium difficile* toxin gene expression. Molecular Microbiology. **79**(4):882-99.

Asen, I., S. Djuranovic, A. N. Lupas, and K. Zeth. 2009. Crystal Structure of SpoVT, the Final Modulator of Gene Expression during Spore Development in *Bacillus subtilis*. Journal of Molecular Biology. **386**: 962–975.

Atomi, H., T. Imanaka, and T. Fukui. 2012. Overview of the genetic tools in the Archaea. Frontiers in Microbiology - Evolutionary and Genomic Microbiology. **3**(337): 1-13.

Bakker, D., W. K. Smits, E. J. Kuijper, and J. Corver. 2012. TcdC does not significantly repress toxin expression in *Clostridium difficile* 630DeltaErm. PLoS One. **7**: e43247.

Bouillaut, L., T. Dubois, A. L. Sonenshein, and B. Dupuy. 2015. Integration of metabolism and virulence in *Clostridium difficile*. Research in Microbiology. **166**(4): 375-83.

Braun, V., T. Hundsberger, P. Leukel, M. Sauerborn, and C. von Eichel-Streiber. 1996. Definition of the single integration site of the pathogenicity locus in *Clostridium difficile*. Gene. **181**: 29–38.

Buffie, C. G., V. Bucci, R. R. Stein, P. T. McKenney, L. Ling, A. Gobourne, D. No, H. Liu, M. Kinnebrew, A. Viale, E. Littmann, M. R. M. van den Brink, R. R. Jenq, Y. Taur, C. Sander, J. R. Cross, N. C. Toussaint, J. B. Xavier, and E. G. Pamer.

2015. Precision microbiome reconstitution restores bile acid mediated resistance to *Clostridium difficile*. Nature. **517**: 205–208.

Burns, D. A., J. T. Heap, and N. P. Minton. 2010. The diverse sporulation characteristics of *Clostridium difficile* clinical isolates are not associated with type. Anaerobe. **16**: 618–622.

Carter, G. P., J. L. Rood, and D. Lyras. 2012. The role of toxin A and toxin B in the virulence of *Clostridium difficile*. Trends in Microbiology. **20**(1): 21-9.

Carter, G. P., G. R. Douce, R. Govind, P. M. Howarth, K. E. Mackin, J. Spencer, A. M. Buckley, A. Antunes, D. Kotsanas, G. A. Jenkin, B. Dupuy, J. I. Rood, and D. Lyras. 2011. The anti-sigma factor TcdC modulates hypervirulence in an epidemic BI/NAP1/027 clinical isolate of *Clostridium difficile*. PLoS Pathogens. **7**:e1002317.

Cartman, S. T., J. T. Heap, S. A. Kuehne, A. Cockayne, and N. P. Minton. 2010. The emergence of 'hypervirulence' in *Clostridium difficile*. International Journal of Medical Microbiology. **300**(6): 387-95.

Cartman, S. T., M. L. Kelly, D. Heeg, J. T. Heap, and N. P. Minton. 2012. Precise manipulation of the *Clostridium difficile* chromosome reveals a lack of association between the tcdC genotype and toxin production. Applied and Environment Microbiology, **78**: 4683–4690.

Cote, C. K., C. A. Rossi, A. S. Kang, P. R. Morrow, J. S. Lee, and S. L. Welkos. 2005. The detection of protective antigen (PA) associated with spores of *Bacillus anthracis* and the effects of anti-PA antibodies on spore germination and macrophage interactions. Microbial Pathogenesis. **38**: 209–225.

Couesnon, A., S. Raffestin, and M. Popoff. 2006. Expression of botulinum neurotoxins A and E, and associated non-toxin genes, during the transition phase and stability at high temperature: analysis by quantitative reverse transcription-PCR. Microbiology. **152**: 759–770.

Curry, S. R., J. W. Marsh, C. A. Muto, M. M. O'Leary, A. W. Pasculle, and L. H. Harrison. 2007. *tcdC* genotypes associated with severe TcdC truncation in an epidemic clone and other strains of *Clostridium difficile*. Journal of Clinical Microbiology. **45**: 215–221.

de Hoon, M. J., P. Eichenberger, D. Vitkup. 2010. Hierarchical evolution of the bacterial sporulation network. Current Biology. **20**: R735–745.

Deakin, L. J., S. Clare, R. P. Fagan, L. F. Dawson, D. J. Pickard, M. R. West, B. W. Wren, N. F. Fairweather, G. Dougan, and T. D. Lawley. 2012. The *Clostridium difficile spo0A* gene is a persistence and transmission factor. Infecttion and Immunity. **80**: 2704–2711.

Debast, S. B., M. P. Bauer, and E. J. Kuijper. 2014. European Society of Clinical Microbiology and Infectious Diseases: Update of the treatment guidance document for *Clostridium difficile* infection. Clinical Microbiology and Infection. **20(**S2):1–26

Deneve, C., C. Janoir, I, Poilane, C. Fantinato, and A. Collignon. 2009. New trends in *Clostridium difficile* virulence and pathogenesis. International Journal of Antimicrobial Agents. **33**(S1): S24–S28.

Dineen, S. S., A. C. Villapakkam, J. T. Nordman, and A. L. Sonenshein AL. 2007. Repression of *Clostridium difficile* toxin gene expression by CodY. Molecular Microbiology. **66**: 206–219.

Dineen, S. S., S. M. McBride, and A. L. Sonenshein. 2010. Integration of metabolism and virulence by *Clostridium difficile* CodY. Journal of Bacteriology. **192**: 5350–5362.

Dong, T. C., S. M. Cutting, and R. J. Lewis. 2004. DNA-binding studies on the *Bacillus subtilis* transcriptional regulator and AbrB homologue, SpoVT. FEMS Microbiology Letters. **233**: 247–256.

Donta S. T., N. Sullivan, and T. D. Wilkins. 1982. Differential Effects of *Clostridium difficile* Toxins on Tissue-Cultured Cells. Journal of Clinical Microbiology. **15**(6): 1157–1158.

Drudy, D., N. Harnedy, S. Fanning, M. Hannan, and L. Kyne. 2007. Emergence and control of fluoroquinolone-resistant, toxin A-negative, toxin B-positive *Clostridium difficile*. Infection Control and Hospital Epidemiology. **28**: 932–940.

Drudy, D., S. Fanning, and L. Kyne. 2007. Toxin A-negative, toxin B-positive *Clostridium difficile*. International Journal of Infecttious Diseases. **11**: 5–10.

Dupuy, B., and A. L. Sonenshein. 1998. Regulated transcription of *Clostridium difficile* toxin genes. Molecular Microbiology. **27**:107–120.

Dworczyński, A., B. Sokół, and F. Meisel-Mikołajczyk. 1991. Antibiotic resistance of *Clostridium difficile* isolates. Cytobios. **65**(262-263): 149-53.

Egerer, M., T. Giesemann, T. Jank, K. J. Satchell, and K. Aktories. 2007. Auto-catalytic cleavage of *Clostridium difficile* toxins A and B depends on cysteine protease activity. Journal of Biological Chemistry. **282**: 25314–2532.

El Meouche, I., J. Peltier, M. Monot, O. Soutourina, M. Pestel-Caron, B. Dupuy, and J. L. Pons. 2013. Characterization of the SigD regulon of *C. difficile* and its positive control of toxin production through the regulation of *tcdR*. PLoS One. **8**: e83748.

Fimlaid, K. A., J. P. Bond, K. C. Schutz, E. E. Putnam, J. M. Leung, T. D. Lawley, and A. Shen. 2013. Global analysis of the sporulation pathway of *Clostridium difficile*. PLoS Genetics. **9**(8): e1003660.

Florin, I., and M. Thelestam. 1983. Internalization of *Clostridium difficile* cytotoxin into cultured human lung fibroblasts. Biochimica et Biophysica Acta. **763**: 383–392.

Galperin, M. Y., S. L. Mekhedov, P. Puigbo, S. Smirnov, Y. I. Wolf, and D. J. Rigden. 2012. Genomic determinants of sporulation in Bacilli and Clostridia: towards the minimal set of sporulation-specific genes. Environmental Microbiology. **14**: 2870–2890.

Gaynes, R., D. Rimland, E. Killum, H. K. Lowery, T. M. 2nd Johnson, G. Killgore, and F. C. Tenover. 2004. Outbreak of *Clostridium difficile* infection in a long-term care facility: association with gatifloxacin use. Clinical Infectious Diseases. **38**: 640–645.

Genth, H., K. Aktories, and I. Just. 1999. Monoglucosylation of RhoA at Threonine37 blocks cytosol-membrane cycling. Journal of Biological Chemistry. **274**: 29050–29056.

Genth, H., S. C. Dreger, J. Huelsenbeck, and I. Just. 2008. *Clostridium difficile* toxins: more than mere inhibitors of Rho proteins. International Journal of Biochemistry and Cell Biology. **40**(4): 592-7.

Giel, J. L., J. A. Sorg, A. L. Sonenshein, and J. Zhu. 2010. Metabolism of bile salts in mice influences spore germination in *Clostridium difficile*. PloS one. **5**(1): e8740

Giesemann, T., T. Jank, R. Gerhard, E. Maier, I. Just, R. Benz, and K. Aktories. 2006. Cholesterol-dependent pore formation of *Clostridium difficile* toxin A. Journal of Biological Chemistry. **281**: 10808–10815.

Govind, R., and B. Dupuy. 2012. Secretion of *Clostridium difficile* Toxins A and B Requires the Holin-like Protein TcdE. PLoS Pathogens. **8**(6): e1002727.

Govind, R., G. Vediyappan, R. D. Rolfe, and J. A. Fralick. 2006. Evidence that *Clostridium difficile* TcdC is a membrane-associated protein. Journal of Bacteriology. **188**: 3716–3720.

Hammond, G. A., and J. L. Johnson. 1995. The toxigenic element of *Clostridium difficile* strain VPI 10463. Microbial Pathogenesis. **19**: 203–213.

Heap, J. T., O. J. Pennington, S. T. Cartman, G. P. Carter, and N. P. Minton. 2007. The ClosTron: a universal gene knock-out system for the genus *Clostridium*. Journal of Microbiological Methods. **70**: 452–464.

Heap, J. T., S. A. Kuehne, M. Ehsaan, S. T. Cartman, C. M. Cooksley, J. C. Scott, and N. P. Minton. 2010. The ClosTron: Mutagenesis in *Clostridium* refined and streamlined. Journal of Microbiological Methods. **80**: 49–55.

Heap, J. T., M. Ehsaan, C. M. Cooksley, Y. K. Ng, S. T. Cartman, K. Winzer, and N. P. Minton. 2012. Integration of DNA into bacterial chromosomes from plasmids without a counter-selection marker. Nucleic Acids Research. **40**(8): e59.

Henriques, A. O., and C. P. Jr. Moran. 2007. Structure, assembly, and function of the spore surface layers. Annual Review of Microbiology. **61**: 555–588.

Herrmann, C., M. R. Ahmadian, F. Hofmann, and I. Just. 1998. Functional consequences of monoglucosylation of H-Ras at effector domain amino acid threonine-35. Journal of Biological Chemistry. **273**: 16134–16139.

Higgins, D., and J. Dworkin. 2012. Recent progress in *Bacillus subtilis* sporulation. FEMS Microbiology Reviews. **36**: 131–148.

Hilbert, D. W., and P. J. Piggot. 2004. Compartmentalization of gene expression *during Bacillus subtilis* spore formation. Microbiology and Molecular Biology Reviews. **68**: 234–262.

Hundsberger, T., V. Braun, M. Weidmann, P. Leukel, M. Sauerborn, and C. von Eichel-Streiber. 1997. Transcription analysis of the genes *tcdA-E* of the pathogenicity locus of *Clostridium difficile*. European Journal of Biochemistry. **244**: 735–742.

Hussain, H. A., A. P. Roberts, and P. Mullany. 2005 Generation of an erythromycin-sensitive derivative of *Clostridium difficile* strain 630 (630Δ*erm*) and demonstration that the conjugative transposon Tn*916*Δ*E* enters the genome of this strain at multiple sites. Journal of Medical Microbiology. **54**: 137-141.

Jank, T., T. Giesemann, and K. Aktories. 2007. Rho-glucosylating *Clostridium difficile* toxins A and B: new insights into structure and function. Glycobiology. **17**: 15R–22R.

Jernberg, C., S. Löfmark, C. Edlund, and J. K. Jansson. 2010. Long-term impacts of antibiotic exposure on the human intestinal microbiota. Microbiology. **156**: 3216–3223.

Johnson, S., M. H. Samore, K. A. Farrow, G. E. Killgore, F. C. Tenover, D. Lyras, J. I. Rood, P. DeGirolami, A. L. Baltch, M. E. Rafferty, S. M. Pear, and D. N. Gerding. 1999. Epidemics of diarrhea caused by a clindamycin-resistant strain of *Clostridium difficile* in four hospitals. New England Journal of Medicine. **341**: 1645–1651.

Just, I., and R. Gerhard. 2004. Large clostridial cytotoxins. Review of Physiology, Biochemistry and Pharmacology. **152**: 23–47.

Just, I., J. Selzer, M. Wilm, C. von Eichel-Streiber, M. Mann, and K. Aktories. 1995. Glucosylation of Rho proteins by *Clostridium difficile* toxin B. Nature. **375**: 500–503.

Karasawa, T., S. Ikoma, K. Yamakawa, and S. Nakamura. 1995. A defined growth medium for *Clostridium difficile*. Microbiology. **141**(Pt 2): 371-5.

Karlsson, S., A. Lindberg, E. Norin, L. G. Burman, and T. Akerlund. 2000. Toxins, butyric acid, and other short-chain fatty acids are coordinately expressed and down-regulated by cysteine in *Clostridium difficile*. Infection and Immunity. **68**: 5881–5888.

Karlsson, S., B. Dupuy, K. Mukherjee, E. Norin, L. G. Burman, and T. Akerlund. 2003. Expression of *Clostridium difficile* Toxins A and B and their sigma factor TcdD is controlled by temperature. Infection and Immunity. **71**: 1784–1793.

Kuehne, S. A., S. T. Cartman, J. T. Heap, M. L. Kelly, A. Cockayne, and N. P. Minton. 2010. The role of toxin A and toxin B in *Clostridium difficile* infection. Nature. **467**(7316): 711-3.

LaFrancea, M. E., M. A. Farrowb, R. Chandrasekaranb, J. Shengc, D. H. Rubinb, and D. B. Lacy. 2015. Identification of an epithelial cell receptor responsible for *Clostridium difficile* TcdB-induced cytotoxicity. PNAS. **112**(22): 7073-7078.

Lanis, J. M., L. D. Heinlen, J. A. James, and J. D. Ballard. 2013. *Clostridium difficile* 027/BI/NAP1 Encodes a Hypertoxic and Antigenically Variable Form of TcdB. PLoS Pathogens. **9**(8): e1003523.

Liyanage, H., S. Kashket, M. Young, and E. R. Kashket. 2001. *Clostridium beijerinckii* and *Clostridium difficile* detoxify methylglyoxal by a novel mechanism involving glycerol dehydrogenase. Applied Environmental Microbiology. **67**: 2004–2010.

Loo, V. G., L. Poirier, M. A. Miller, M. Oughton, M. D. Libman, S. Michaud, A. M. Bourgault, T. Nguyen, C. Frenette, M. Kelly, A. Vibien, P. Brassard, S. Fenn, K. Dewar, T. J. Hudson, R. Horn, P. René, Y. Monczak, and A. Dascal. 2005. A predominantly clonal multiinstitutional outbreak of *Clostridium difficile* associated diarrhea with high morbidity and mortality. New England Journal of Medicine. **353**: 2442–2449.

Lyras, D., J. R. O'Connor, P. M. Howarth, S. P. Sambol, G. P. Carter, T. Phumoonna, R. Poon, V. Adams, G. Vedantam, S. Johnson, D. N. Gerding, and J. L. Rood. 2009. Toxin B is essential for virulence of *Clostridium difficile*. Nature. **458**: 1176–1179.

Mackin, K. E., G. P. Carter, P. Howarth, J. L. Rood, and D. Lyras. 2013. Spo0A differentially regulates toxin production in evolutionarily diverse strains of *Clostridium difficile*. PLoS One. **8**(11): e79666.

Mani, N., and B. Dupuy. 2001. Regulation of toxin synthesis in *Clostridium difficile* by an alternative RNA polymerase sigma factor. PNAS U S A. **98**(10): 5844-9.

Mani, N., D. Lyras, L. Barroso, P. Howarth, T. Wilkins, J. I. Rood, A. L. Sonenshein, and B. Dupuy. 2002. Environmental response and autoregulation of *Clostridium difficile* TxeR, a sigma factor for toxin gene expression. Journal of Bacteriology. **184**: 5971–5978.

Matamouros, S., P. England, and B. Dupuy. 2007. *Clostridium difficile* toxin expression is inhibited by the novel regulator TcdC. Molecular Microbiology. **64**: 1274–1288.

Matsuoka, K., S. Mizuno, A. Hayashi, T. Hisamatsu, M. Naganuma, and T. Kanai. 2014. Fecal Microbiota Transplantation for Gastrointestinal Diseases. Keio Journal of Medicine. **63**(4): 69–74.

McDonald, L. C., G. E. Killgore, and A. Thompson. 2005. An epidemic, toxin gene-variant strain of *Clostridium difficile*. New England Journal of Medicine. **353**(23): 2433–2441.

McFarland, L. V., H. W. Beneda, J. E. Clarridge, and G. J. Raugi. 2007. Implications of the changing face of *Clostridium difficile* disease for health care practitioners. American Journal of Infection control. **35**(4): 237-253.

McKee, R. W., M. R. Mangalea, E. B. Purcell, E. K. Borchardt, and R. Tamayo. 2013. The second messenger cyclic Di-GMP regulates *Clostridium difficile* toxin production by controlling expression of *sigD*. Journal of Bacteriology. **195**(22): 5174-85.

McKenney, P. T., A. Driks, and P. Eichenberger. 2012. The *Bacillus subtilis* endospore: assembly and functions of the multilayered coat. Nature Reviews Microbiology. **11**: 33–44.

Merrigan, M., A. Venugopal, M. Mallozzi, B. Roxas, V. K. Viswanathan, S. Johnson, D. N. Gerding, and G. Vedantam. 2010. Human hypervirulent *Clostridium difficile* strains exhibit increased sporulation as well as robust toxin production. Journal of Bacteriology. **192**(19): 4904-11.

Miller, D. A., G. Suen, K. D. Clements, and E. R. Angert. 2012. The genomic basis for the evolution of a novel form of cellular reproduction in the bacterium *Epulopiscium*. BMC Genomics. **13**: 265.

Molle, V., M. Fujita, S. T. Jensen, P. Eichenberger, J. E. Gonzalez-Pastor, J. S. Liu, and R. Losick. 2003. The Spo0A regulon of *Bacillus subtilis*. Molecular Microbiology. **50**: 1683–1701.

Moncrief, J. S., L. A. Barroso, and T. D. Wilkins. 1997. Positive regulation of *Clostridium difficile* toxins. Infection and Immunity. **65**: 1105–1108.

Moncrief, J. S., and T. D. Wilkins. 2000. Genetics of *Clostridium difficile* Toxins. Coordinating ed., K. Aktories. Springer-Verlag Berlin Heidelberg. Virginia.

Muto, C. A., M. Pokrywka, K. Shutt, A. B. Mendelsohn, K. Nouri, K. Posey, T. Roberts, K. Croyle, S. Krystofiak, S. Patel-Brown, A. W. Pasculle, D. L. Paterson, M. Saul, and L. H. Harrison. 2005. A large outbreak of *Clostridium difficile*-associated disease with an unexpected proportion of deaths and colectomies at a teaching hospital following increased fluoroquinolone use. Infection Control and Hospital Epidemiology. **26**: 273–280.

Na, X., H. Kim, M. P. Moyer, C. Pothoulakis, and J. T. LaMont. 2008. gp96 is a human colonocyte plasma membrane binding protein for *Clostridium difficile* toxin A. Infection and Immunity. **76**(7): 2862-71.

Ng, Y. K., M. Ehsaan, S. Philip, M. M. Collery, C. Janoir, A. Collignon, S. T. Cartman, and N. P. Minton. 2013. Expanding the Repertoire of Gene Tools for Precise Manipulation of the *Clostridium difficile* Genome: Allelic Exchange Using *pyrE* Alleles. PloS One. **8**: e56051.

O'Connor, J. R., D. Lyras, K. A. Farrow, V. Adams, D. R. Powell, J. Hinds, J. K. Cheung, and J. I. Rood. 2006. Construction and analysis of chromosomal *Clostridium difficile* mutants. Molecular Microbiology. **61**: 1335–1351.

Ohtani, K., H. Hirakawa, D. Paredes-Sabja, K. Tashiro, S. Kuhara, M. R. Sarker, T. Shimizu. 2013. Unique regulatory mechanism of sporulation and enterotoxin production in *Clostridium perfringens*. Journal of Bacteriology. **195**(12): 2931-6.

Oliva, C., C. L. Jr. Turnbough, and J. F. Kearney. 2009. CD14-Mac-1 interactions in *Bacillus anthracis* spore internalization by macrophages. PNAS U S A. **106**: 13957–13962.

Olling, A., S. Seehase, N. P. Minton, H. Tatge, S. Schröter, S. Kohlscheen, A. Pich, A., I. Just, R. Gerhard. 2012. Release of TcdA and TcdB from *Clostridium difficile* cdi 630 is not affected by functional inactivation of the *tcdE* gene. Microbial Pathogenesis. **52**(1): 92-100.

Onderdonk, A. B., B. R. Lowe, and J. G. Bartlett. 1979. Effect of environmental stress on *Clostridium difficile* toxin levels during continuous cultivation. Applied and Environmental Microbiology. **38**: 637–641.

Panessa-Warren, B. J., G. T. Tortora, and J. B. Warren. 2007. High resolution FESEM and TEM reveal bacterial spore attachment. Microscopy and Microanalysis. **13**: 251–266.

Paredes, C. J., K. V. Alsaker, and E. T. Papoutsakis. 2005. A comparative genomic view of clostridial sporulation and physiology. Nature Review Microbiology. **3**: 969–978.

Paredes-Sabja, D., and M. R. Sarker. 2012. Adherence of *Clostridium difficile* spores to Caco-2 cells in culture. Journal of Medical Microbiology. **61**: 1208–1218.

Paredes-Sabja, D., G. Cofre-Araneda, C. Brito-Silva, M. Pizarro-Guajardo, and M. R. Sarker. 2012. *Clostridium difficile* spore-macrophage interactions: spore survival. PLoS One. **7**: e43635.

Peláez, T., R. Sanchez, R. Blazquez, P. Catalan, P. Munoz, and E. Bouza. 1994. Metronidazole resistance in *Clostridium difficile*: A new emerging problem? Abstract E-

34:50. Program and Abstracts of the 34th Interscience Conference on Antimicrobial Agents and Chemotherapy (ICAAC). Orlando, FL.

Pépin, J., N. Saheb, M. A. Coulombe, M. E. Alary, M. P. Corriveau, S. Authier, M. Leblanc, G. Rivard, M. Bettez, V. Primeau, M. Nguyen, C. E. Jacob, and L. Lanthier. 2005. Emergence of fluoroquinolones as the predominant risk factor for *Clostridium difficile* associated diarrhea: a cohort study during an epidemic in Quebec. Clinical Infectious Diseases. **41**: 1254–1260.

Pereira, F. C., L. Saujet, A. R. Tomé, M. Serrano, M. Monot, E. Couture-Tosi, I. Martin-Verstraete, B. Dupuy, and A. O. Henriques. 2013. The Spore Differentiation Pathway in the Enteric Pathogen *C. difficile*. PLOS genetics. **9**(10): e1003782.

Pérez-Cobas, A. E., M. J. Gosalbes, A. Friedrichs, H. Knecht, A. Artacho, K. Eismann, W. Otto, D. Rojo, R. Bargiela, M. von Bergen, S. C. Neulinger, C. Däumer, F. A. Heinsen, A. Latorre, C. Barbas, J. Seifert, V. M. dos Santos, S. J. Ott, M. Ferrer, and A. Moya. 2013a. Gut microbiota disturbance during antibiotic therapy: a multi-omic approach. Gut. **62**: 1591–1601.

Permpoonpattana, P., E. H. Tolls, R. Nadem, S. Tan, A. Brisson, S. M. Cutting. 2011. Surface Layers of *Clostridium difficile* Endospores. Journal of Bacteriology. **193**(23): 6461–6470.

Piggot, P. J., and D. W. Hilbert. 2004. Sporulation of *Bacillus subtilis*. Current Opinion in Microbiology. **7**: 579–586.

Purdy, D., T. A. O'Keeffe, M. Elmore, M. Herbert, A. McLeod, M. Bokori-Brown, A. Ostrowski, and N. P. Minton. 2002. Conjugative transfer of clostridial shuttle vectors from *Escherichia coli* to *Clostridium difficile* through circumvention of the restriction barrier. Molecular Microbiology. **46**(2): 439-52.

Rodriguez-Palacios, A., H. R. Stämpfli, T. Duffield, A. S. Peregrine, L. A. Trotz-Williams, L. G. Arroyo, J. S. Brazier, and J. S. Weese. 2006. *Clostridium difficile* PCR ribotypes in calves, Canada. Emerging Infectious Diseases. **12**: 1730–1736.

Rosenbusch, K. E., D. Bakker, E. J. Kuijper, and W. K. Smits. 2012. *C. difficile* 630Δ*erm* Spo0A regulates sporulation, but does not contribute to toxin production, by direct high-affinity binding to target DNA. PLoS One. **7**(10): e48608.

Rupnik, M. 2007. Is *Clostridium difficile*-associated infection a potentially zoonotic and foodborne disease? Clinical Microbiology and Infection. **13**: 457–459.

Rupnik, M., M. H. Wilcox, and D. N. Gerding. 2009. *Clostridium difficile* infection: new developments in epidemiology and pathogenesis. Nature Reviews Microbiology. **7**: 526-36.

Sambrook, J., and M. R. Green. 2012. *Molecular Cloning*: A Laboratory Manual. Coordinating ed., J. Inglis 4 ed. Cold Spring Harbor Laboratory Press. New York.

Sarker, M. R., D. Paredes-Sabja. 2012. Molecular basis of early stages of *Clostridium difficile* infection: germination and colonization. Future Microbiology. **7**: 933–943.

Saujet, L., M. Monot, B. Dupuy, O. Soutourina, I. Martin-Verstraete. 2011. The key sigma factor of transition phase, SigH, controls sporulation, metabolism, and virulence factor expression in *Clostridium difficile*. Journal of Bacteriology. **193**(13): 3186-96.

Saujet, L., F. C. Pereira, M. Serrano, O. Soutourina, M. Monot, P. V. Shelyakin, M. S. Gelfand, B. Dupuy, A. O. Henriques, and I. Martin-Verstraete. 2013. Genome-wide analysis of cell type-specific gene transcription during spore formation in *Clostridium difficile*. PLoS Genetics. **9**(10): e1003756.

Schorch, B., S. Song, F. R. van Diemen, H. H. Bock, P. May, J. Herz, T. R. Brummelkamp, P. Papatheodorou, and K. Aktories. 2014. LRP1 is a receptor for *Clostridium perfringens* TpeL toxin indicating a two-receptor model of clostridial glycosylating toxins. PNAS USA. **111**(17): 6431–6436.

Sehr, P., G. Joseph, H. Genth, I. Just, E. Pick, and K. Aktories. 1998. Glucosylation and ADP-ribosylation of Rho proteins—effects on nucleotide binding, GTPase activity, and effector-coupling. Biochemistry. **37**: 5296–5304.

Serrano, M., G. Real, J. Santos, J. Carneiro, C. P. Jr. Moran, and A.O. Henriques. 2011. A negative feedback loop that limits the ectopic activation of a cell type-specific sporulation sigma factor of *Bacillus subtilis*. PLoS Genetics. **9**:e1002220.

Songer, G. J., and M. A. Anderson. 2006. *Clostridium difficile*: an important pathogen of food animals. Anaerobe. **12**: 1-4.

Sorg, J. A. and Sonenshein, A. L. 2008b. Bile salts and glycine as cogerminants for *Clostridium difficile* spores. Journal of bacteriology. **190**(7): 2505-2512

Sorg, J. A., and A. L. Sonenshein. 2008a. Chenodeoxycholate is an inhibitor of *Clostridium difficile* spore germination. Journal of bacteriology. **191**(3): 1115-1117

Steichen, C., P. Chen, J. F. Kearney, and C. L. Jr. Turnbough. 2003. Identification of the immunodominant protein and other proteins of the *Bacillus anthracis* exosporium. Journal of Bacteriology. **185**(6)**:** 1903-10.

Stragier, P. 2002. A gene odyssey: exploring the genomes of endospore-forming bacteria, p. 519–525. Coordinating ed., Sonenshein, Losick, Hoch. ASM PressIn: AL S, editor. *Bacillus subtilis* and its closest relatives: from genes to cells. Washington, DC ASM.

Sylvestre, P., E. Couture-Tosi, and M. Mock. 2002. A collagen-like surface glycoprotein is a structural component of the *Bacillus anthracis* exosporium. Molecular Microbiology. **45**(1): 169-78.

Sylvestre, P., E. Couture-Tosi, and M. Mock. 2003. Polymorphism in the collagen-like region of the *Bacillus anthracis* BclA protein leads to variation in exosporium filament length. Journal of Bacteriology. **185**(5): 1555-63.

Tan, K. S., B. Y. Wee, and K. P. Song. 2001. Evidence for holin function of *tcdE* gene in the pathogenicity of *Clostridium difficile*. Journal of Medical Microbiology. **50**: 613–619.

Thelestam, M., and E. Chaves-Olarte. 2000. Cytotoxic effects of the *Clostridium difficile* toxins. Current Topics in Microbiology and Immunology. **250**: 85–96.

Traag, B. A., A. Pugliese, J. A. Eisen, and R. Losick. 2012. Gene conservation among endospore-forming bacteria reveals additional sporulation genes in *Bacillus subtilis*. Journal of Bacteriology. **195**(2): 253–60.

Underwood, S., S. Guan, V. Vijayasubhash, S. Baines, L. Graham, R. Lewis, M. Wilcox, and K. Stephenson. 2009. Characterization of the Sporulation Initiation Pathway of *Clostridium difficile* and Its Role in Toxin Production. Journal of Bacteriology**. 191**(23): 7296–7305.

van Leeuwen, H. C., D. Bakker, P. Steindel, E. J. Kuijper, and J. Corver. 2013. *Clostridium difficile* TcdC protein binds four-stranded G-quadruplex structures. Nucleic Acids Research. **41**: 2382–2393.

Vohra, P., and I. R. Poxton. 2011. Comparison of toxin and spore production in clinically relevant strains of *Clostridium difficile*. Microbiology. **157**(Pt 5): 1343-53.

Wang, I. N., D. L. Smith, and R. Young. 2000. Holins: the protein clocks of bacteriophage infections. Annual Review of Microbiology. **54**: 799–825.

Warny, M., J. Pepin, A. Fang, G. Killgore, A. Thompson, J. Brazier, E. Frost, and L. C. McDonald. 2005. Toxin production by an emerging strain of *Clostridium difficile* associated with outbreaks of severe disease in North America and Europe. Lancet. **366**: 1079–1084.

Willing, B. P., S. L. Russell, and B. B. Finlay. 2011. Shifting the balance: antibiotic effects on host-microbiota mutualism. Nature Review Microbiology. **9**: 233–243.

Wilson, K. H. 1983. Efficiency of various bile salt preparations for stimulation of *Clostridium difficile* spore germination. Journal of clinical microbiology. **18**(4): 1017-1019

Wilson, K. H., M. J. Kennedy, and F. R. Fekety. 1982. Use of sodium taurocholate to enhance spore recovery on a medium selective for *Clostridium difficile*. Journal of Clinical Microbiology. **15**: 443–446.

Yamakawa, K., T. Karasawa, S. Ikoma, and S. Nakamura. 1996. Enhancement of *Clostridium difficile* toxin production in biotin-limited conditions. Journal of Medical Microbiology. **44**: 111– 114.

Young, I., I. Wang, and W. D. Roof. 2000. Phages will out: strategies of host cell lysis. Trends in Microbiology. **8**: 120–128.

Zhao, H., T. Msadek, J. Zapf, Madhusudan, J. A. Hoch, and K. I. Varughese. 2002. DNA complexed structure of the key transcription factor initiating development in sporulating bacteria. Structure. **10**(8): 1041-50.

6. Appendix

Appendix 1: *Escherichia coli* strains used in this work

Strain	Genotype	Origin
DH5α	F⁻ Φ80*lac*ZΔM15 Δ(*lac*ZYA*arg*F) U169 *rec*A1 *end*A1 *hsd*R17 (rK–, mK+) *pho*A *sup*E44 λ⁻ *thi*-1 *gyr*A96 *rel*A1	Bethesda Research laboratories
HB101	supE44 *aa*14 *galK*2 *lacY*1 D(*gpt-proA*) 62 *rpsL*20 *(Str*^{R}*)* *xyl*-5 *mtl*-1 *rec*A13 D*(mcrC-mrr) hsd*S_B(r_B-m_B-) RP4	El Meouche *et al.*, 2013
AHCD125	HB101 (pRP4) (pMS464)	Laboratory stock
AHCD144	HB101 (pRP4) (pMS470)	"
AHCD203	HB101 (pRP4) (pMTL-YN1)	Ng *et al.*, 2013
AHCD204	HB101 (pRP4) (pMTL-YN1C)	Ng *et al.*, 2013
AHCD207	HB101 (pRP4) (pMTL-YN3)	Ng *et al.*, 2013
AHCD226	DH5α (pSR3)	This work
AHCD234	DH5α (pSR4)	"
AHCD239	HB101 (pRP4) (pSR3)	"
AHCD240	HB101 (pRP4) (pSR4)	"
AHCD284	DH5α (pSR5)	"
AHCD285	HB101 (pRP4) (pSR5)	"
AHCD342	DH5α (pSR6)	"
AHCD343	HB101 (pRP4) (pSR6)	"

Appendix 2: *Clostridium difficile* strains used in this work

Strain	Genotype	Origin
AHCD531	630Δ*erm*	Hussain *et al.*, 2005
AHCD591	630Δ*erm*Δ*tcdA*Δ*tcdB*	Kuehne *et al.*, 2010
AHCD608	*C. difficile* 630Δ*erm* (pMS464)	Laboratory stock
AHCD668	*C. difficile* 630Δ*erm* (pMS470)	"
AHCD772	630Δ*erm*Δ*pyrE*	Heap *et al.*, 2012.
AHCD811	630Δ*erm*Δ*pyrE*Δ*tcdR*	This work
AHCD820	630Δ*erm*Δ*tcdR*	"
AHCD827	630Δ*erm*Δ*pyrE*Δ*tcdE*	"
AHCD828	630Δ*erm*Δ*tcdR*^{C}	"
AHCD833	630Δ*erm*Δ*tcdE*	"
AHCD840	*C. difficile* 630Δ*erm*Δ*tcdR* (pMS464)	"
AHCD841	*C. difficile* 630Δ*erm*Δ*tcdR* (pMS470)	"
AHCD845	*C. difficile* 630Δ*erm*Δ*tcdR*^{C} (pMS464)	"
AHCD846	*C. difficile* 630Δ*erm*Δ*tcdR*^{C} (pMS470)	"
AHCD872	630Δ*erm*Δ*tcdE*^{C}	"

^{C} - complemented strain

Appendix 3: *C. difficile* minimal medium (Karasawa *et al.*, 1995).

	Volume	Weight (g)	Stock concentration (mg/ml)	Final concentration (mg/ml)
Amino acids (5x)				
Casamino acids	1 L	50	50	10
L-tryptophan		2.5	2.5	0.5
L-Cysteine		2.5	2.5	0.5
Salts (10x)				
Na_2HPO_4	1 L	50	50	5
$NaHCO_3$		50	50	5
KH_2PO4		9	9	0.9
NaCl		9	9	0.9
Glucose (20x)	500 ml			
D-Glucose		100	200	10
Trace salts (50x)				
$(NH_4)_2SO_4$	500 ml	1	2.0	0.04
$CaCl_2.2H_2O$		0.65	1.3	0.026
$MgCl_2.6H_2O$		0.5	1.0	0.02
$MnCl_2.4H_2O$		0.25	0.5	0.01
$CoCl_2.6H_2O$		0.025	0.05	0.001
Iron (100x)	100 ml			
$FeSO_4.7H_2O$		0.04	0.4	0.004
Vitamins				
D-biotin (1000x)	10 ml	0.01	1	0.001
Calcium-D-panthothenate (1000x)		0.01	1	0.001
Pyridoxine (1000x)		0.01	1	0.001

Appendix 4: Primers used in the work

Name	Sequence (5'→3')
tcdE-AscI-Fw	CCC CGG CGC GCC TTG ATG ATA TAA AAT ATT ATT TTG
tcdE-SOE-Rev	TTC CTT TAA TCT CTT AGG CAT ATT CAT AAC GCC TCC TAG
tcdE-SOE-Fw	CCT AAG AGA TTA AAG GAA AAA ATA GC
tcdE-SbfI-Rev	CCC CCC TGC AGG ACT CTT CTA TTA GAT AAG
tcdE-vef-Fw	CAG CAG AAG CAT ATA TAG G
tcdE-vef-Rev	GAG AGT GCT CTA TTT CTG C
tcdE-comp-SacI-Fw	CCC GAG CTC CAATAA AAA GGT GGA CTA TGA TGA
tcdE-comp-BamHI-Rev	CCC GGA TCC TTA CTT TTC ATC CTT AGC
tcdR-AscI-Fw	CCC CGG CGC GCC ATT ATC TTA AGA GAG GAG
tcdR-SOE-Rev	CAT AAA TAA AAT TTC TTG CAA ATC ATC
tcdR-SOE-Fw	TTG CAA GAA ATT TTA TTT ATG GAA AAT TAT TTT AAC TTG
tcdR-SbfI-Rev	CCC CCC TGC AGG TAT CTA TAT AAA TAT CTG
tcdR-vef-Fw	GTA TCA TTT CAC GAA GAG G
tcdR-vef-Rev	GGG TCA TTT AAG TTT TCT C
tcdR-comp-BamHI-Fw	CCC GGA TCC TAA AAA TAT TTT GAT ATG
tcdR-comp-HindIII-Rev	CCC AAG CTT ATT AAT TTG CTC TTC
YN3-vef-Fw	CATCAAGAAGAGCGACTTCG
YN3-vef-Rev	TTCTTTCTATTCAGCACTGTTATGC
pyrE-vef-Fw	CAATAATTTTATAACATTAACATGG
pyrE-vef-Rev	GTGTTACTTAAAAAATGTAAAT

Underlined – Restriction sites

Appendix 5: Plasmids used in this work

Plasmid	Description
pMS464	Plasmid carrying the *tcdR* promoter fused to the $SNAP^{Cd}$-*tag*. Resistance to Thiamphenicol.
pMS470	Plasmid carrying the *tcdA* promoter fused to the $SNAP^{Cd}$-*tag* Resistance to Thiamphenicol.
pFT46	Plasmid carrying a P_{tet}-$SNAP^{Cd}$ transcriptional fusion (Pereira *et al.*, 2013). Resistance to Thiamphenicol.
pMTL-YN3	Plasmid to construct mutants in *C. difficile* 630Δ*erm*Δ*pyrE* using the Allele Coupled Exchange mutagenesis (Ng *et al.*, 2013). Resistance to Thiamphenicol.
pMTL-YN1	Plasmid to revert the *pyrE* gene in *C. difficile* 630Δ*erm*Δ*pyrE* using the Allele Coupled Exchange mutagenesis (Ng *et al.*, 2013). Resistance to Thiamphenicol.
pMTL-YN1C	Plasmid to complement *in trans* and revert the *pyrE* gene of *C. difficile* 630Δ*erm*Δ*pyrE* using the Allele Coupled Exchange mutagenesis (Ng *et al.*, 2013). Resistance to Thiamphenicol.
pSR3	Plasmid used for the *tcdR* mutagenesis of 630Δ*erm*Δ*pyrE strain*. With origin in the pMTL-YN3. Resistance to Thiamphenicol.
pSR4	Plasmid used for the *tcdE* mutagenesis of 630Δ*erm*Δ*pyrE strain*. With origin in the pMTL-YN3. Resistance to Thiamphenicol.
pSR5	Plasmid used to complement *tcdR in trans* and revert the *pyrE* gene of *C. difficile* 630Δ*erm*Δ*pyrE*Δ*tcdR*. With origin in the pMTL-YN1C. Resistance to Thiamphenicol.
pSR6	Plasmid used to complement *tcdE in trans* and revert the *pyrE* gene of *C. difficile* 630Δ*erm*Δ*pyrE*Δ*tcdE*. With origin in the pMTL-YN1C. Resistance to Thiamphenicol.